PEOPLE'S DEMOCRATIC REPUBLIC OF ALGERIA

Ministry of Higher Education and Scientific Research

Echahid Hamma Lakhdar University of El-Oued

FACULTY OF TECHNOLOGIES

DEPARTMENT OF ELECTRICAL ENGINEERING

FINAL STUDY DISSERTATION

In the aim obtaining of

2eme MASTER DEGREE

Domain: Sciences and Technology

Option: Mechanical engineering

Specialty: Electromechanical

THEME

Modeling and Direct Torque Control (DTC) of the Doubly Fed Asynchronous Machine

Presented by:

- BEGUI Mohammed Laid
- NEGHMOUCHE NACER Aymen
- SAYAH Abdelmadjid
- SOUALAH MOHAMMED Abdallah

Supervised by:

- Dr. LARGOT Soulef

Academic year :2023/2024

﴿ رَبَّنَا لاَ تُؤَاخِذْنَا إِن نَّسِينَا أَوْ أَخْطَأْنَا رَبَّنَا وَلاَ تَحْمِلْ عَلَيْنَا إِصْرًا كَمَا حَمَلْتَهُ عَلَى الَّذِينَ مِن قَبْلِنَا رَبَّنَا وَلاَ تُحَمِّلْنَا مَا لاَ طَاقَةَ لَنَا بِهِ وَاعْفُ عَنَّا وَاغْفِرْ لَنَا وَارْحَمْنَا أَنتَ مَوْلاَنَا فَانصُرْنَا عَلَى الْقَوْمِ الْكَافِرِينَ﴾ **سورة البقرة : الآية286 .**

" صدق الله العظيم"

ACKNOWLEDGEMENTS

First of all, I thank God -ALLAH- of the Almighty for having given me courage and patience during all these years of study.

I would like to express my sincere gratitude and thanks to ***Dr. LARGOT Soulef,*** *Doctor at the Echahid Hamma Lakhdar University of El Oued, for having directed this work.*

My sincere thanks to the members of the jury for the honor they have done me by participating in the judging of this work.

We would like to thank warmly all those who helped us to develop and produce this thesis, as well as to all those who helped us in any way to accomplish this work.

Finally, I would like to thank my parents in particular for their unconditional support throughout these long years of study.

DEDICATION

In the name of God the Merciful Praise be to Allah Almighty

We dedicate this humble work as respect, appreciation and thanks:

To our dear fathers, mothers and brothers who helped us from near and far.

To all our family that bears the name of Bebboukha, Mosbahi and Medekhel

To everyone who contributed to the development of this humble work and

All these are dear to us.

Abstract

الملخص

Abstract

In this trail, a study of a DTC control of a doubly fed induction machine (DFIM), through a three, phase two-level converter connected to a stator has been presented. For this purpose, a state of, the art of the studied machine has been carried out. A mathematical model of the machine is presented using MATLAB. The DFIM which is fed by a three phase two-level PWM converter, has been modeled and its control approach has been given. Also, the problem of decoupling, between the flux and the torque has been treated. The simulation results display that the assigned objective has been reached.

Keywords: DFIM, DTC, PWM converter, three phase-two level converter, Matlab.

الملخص

تتناول هذه المذكرة دراسة محرك لا تزامني ثلاثي الطور ثنائي التغذية، ذو عضو دوار ملفوف، بواسطة التحكم المباشر للعزم حيث تتم تغذية العضو الساكن بواسطة مموج ذو مستويين من أجل هذا تما عرض المحرك على الباحثين في هذا المجال، ثم انتقلنا بعد ذلك إلى إعطاء النموذج الرياضي للمحرك. ثم اتبعناه. بعد ذلك بمحاكاة، وبما أن تغذية المحرك تتم عبر مموج ذو مستويين، فقد قمنا بإعطاء النموذج الرياضي وطرق التحكم فيها أما فيما يتعلق بالفصل بين التدفق والعزم، فقد استعملنا التحكم المباشر للعزم الذي يوجها فيها العزم وفق العضو الدوار. حيث بينت نتائج المحاكاة أن الفصل بين التدفق والعزم قد تم فعلا.

الكلمات المفتاحية: محرك لا تزامني، التحكم المباشر للعزم، مموج، المتلاب.

TABLE OF CONTENTS

TABLE OF CONTENTS

Acknowledgements

Dedication

Abstract

Table of contents

List of Figures

List of Tables

General Introduction a

CHAPTER I

State of the art of the doubly fed induction machine (DFIM)

I.1. Introduction 4

I.2. Description of the doubly fed induction machine 4

I.2.1. Stator 5

I.2.2. Rotor 5

I.2.3. Slip Rings and Brushes 6

I.2.4. Power Electronics 6

I.2.5. Variable Speed Operation 6

I.2.6. Bidirectional Power Flow 6

I.3. Classification of the doubly fed induction machine 6

I.3.1. Single doubly fed machine 6

I.3.2. Cascaded Doubly Fed Induction Machine 7

I.3.3. Single Frame Cascaded Doubly Fed Induction Machine 7

I.3.4. Doubly Fed Machine Without Collector 8

I.3.5. Brushless Doubly Fed Induction Machine 8

I.4. Operating principle of DFIM 9

I.5. Operating modes of DFIM 9

I.5.1. Motoring at Sub-synchronous Speed 10

I.5.2. Motoring at Super-synchronous Speed 11

I.5.3. Generating at Sub-synchronous Speed 11

I.5.4. Generating at Super-synchronous Speed 12

I.6. Operation in hyper-synchronous generator mode 12

I.6.1. Variable frequency drive 13
I.6.1.1. Scalar control 13
I.6.1.2. Vector control 13
I.6.2. Nonlinear control techniques 13
I.6.2.1. Feed-back linearization 13
I.6.2.2. Sliding mode control 14
I.6.3. Sensorless control techniques 14
I.7. Areas of application of DFIM 14
I.8. Advantages and disadvantages of DFIM 15
I.8.1. Advantages of DFIM 15
I.8.2. Disadvantages of DFIM 16
I.9.Conclusion 17

CHAPTER II

Modeling of the doubly fed induction machine

II.1. Introduction 19
II.2. Three-phase model of DFIM 20
II.2.1. Description 20
II.2.2. Hypothèse 20
II.2.3. Actual Electrical Equations of the Machine 21
II.2.4. Magnetic Equations 21
II.3. Two-phase modelling of DFIM 22
II.3.1. Application of the Park Transformation 22
II.3.1.1. Electrical equations 23
II.3.1.2. Magnetic equations 24
II.3.1.3. The electromagnetic torque 26
II.3.2. Choice of Park's frame of reference 27
II.4. Model of the DFIM in the form of an equation of state 28
II.5. Modelling of the power system 29
II.5.1. The structure of the supply chain chosen 29
II.5.2. Modeling of a three-phase double-alternating diode rectifier 30
II.5.3. Modelling of the filter circuit 31
II.5.4. Modeling of the Voltage Inverter 32
II.6. Simulation of the DFIM 35
II.6.1. DFIM Simulation Results 36

II.6.2. Simulation of the DFIM association with PWM inverter 37
II.6.3. Simulation results 38
II.7. Conclusion 39

CHAPTER III

Direct Torque Control (DTC) of the doubly fed induction machine

III.1.Introduction 40
III.2. General Structure of The DTC 40
III.3. Principle of the DTC order 41
III.4. Operation of a three-phase voltage inverter 42
III.5. Control of stator flow and electromagnetic torque 44
III.5.1. Principle of Stator Flow Control 44
III.5.2. Electromagnetic torque control principle 45
III.6. Choosing the voltage vector 46
III.7. Estimators 47
III.7.1. Estimation of stator flux 47
III.7.2. Electromagnetic torque estimation 49
III.8. Elaboration of the control vector 49
III.8.1. Flow corrector 49
III.8.2. Torque corrector 50
III.8.3. Two-level corrector 50
III.8.4. Three-level corrector 51
III.8.5. Elaboration of the commutation table 52
III.9.Conclusion 53

Chapter IV

Direct Torque Control simulation

IV.1. Introduction 55
IV.2. General structure of direct torque control 56
IV.2.1. DFIM DTC simulation results 56
IV.2.2. Variation of speed and load torque 56
IV.2.3. Empty start 57
IV.2.4. Interpretation of results 58
IV.2.5. 1-charge start-up 59
IV.2.6. Interpretation of results 60
IV.2.7. 3-charge start-up 61

IV.2.8. Interpretation of results: 62
IV.3. Conclusion 63
General conclusion 65
Appendix
Bibliography

List of Figures

LIST OF FIGURES

Page

CHAPTER I

State of the art of the doubly fed induction machine (DFIM)

Figure 1 *Construction of Induction Motor* 4

Figure 2 *An overview of the stator structure* 5

Figure 3 *Stator composition* 5

Figure 4 *Squirrel Cage Rotor Vs Wound Rotor* 5

Figure 5 *Schematic Diagram of Single doubly fed machine* 7

Figure 6 *Schematic Diagram of Cascaded Doubly Fed Induction Machine* 7

Figure 7 *Schematic Diagram of Single Frame Cascaded Doubly Fed Induction Machine* 8

Figure 8 *Schematic Diagram of Doubly Fed machine without collector* 8

Figure 9 *Schematic Diagram of Brushless Doubly Fed Induction Machine* 9

Figure 10 *Operational modes characteristic of the DFIM* 10

Figure 11 *Operation in hypo-synchronous motor mode* 10

Figure 12 *Operation in hyper-synchronous motor mode* 11

Figure 13 *Operation in hypo-synchronous generator mode* 11

Figure 14 *Operation in hyper-synchronous generator mode* 12

Figure 15 *Diagram of the different control strategies of an IM* 12

CHAPTER II

Modeling of the doubly fed induction machine

Figure 1 *Schematic representation of the DFIM* 20

Figure 2 *Spatial position of the different reference frames* 22

Figure 3 *Representation of d-axis and q-axis dummy windings* 26

Figure 4 *Proposed synoptic diagram for feeding the DFIM* 30

Figure 5 *Diagram of a three-phase double-alternating diode rectifier* 30

Figure 6 *Rectified Voltage Filter Circuit* 31

Figure 7 *Two-Level Three-Phase Voltage Inverter* 32

Figure 8 *Representation of a GTO* 32

Figure 9 *DFIM Simulation Structure* 35

Figure 10 *DFIM simulation block diagram* 35

Figure 11 *DFIM Simulation Results* 36

Figure 12 *Diagram of the DFIM simulation block with PWM inverter* 37
Figure 13 *Results of MADA Simulation with PWM Inverter* 38
Figure 14 *Impurities at speed* 39
Figure 15 *Impurities at torque* 39

CHAPTER III

Direct Torque Control (DTC) of the doubly fed induction machine

Figure 1 *General Structure of The DTC* 40
Figure 2 *Principle of the DTC order* 42
Figure 3 *Asynchronous machine controlled by voltage inverter* 42
Figure 4 *Operating Sequences of a Two-Level Voltage Inverter* 43
Figure 5 *Evolution of stator flux vector in the complex* 44
Figure 6 *Area Distribution* 47
Figure 7 *Flux corrector with hysteresis and selection of the corresponding voltage vectors.* 50
Figure 8 *Two-level Flux corrector* 51
Figure 9 *Three-level Flux corrector* 51

Chapter IV

Direct Torque Control simulation

Figure 1 *General structure of direct torque control* 56
Figure 2 *Rotational speed* 57
Figure 3 *Electromagnetic torque* 57
Figure 4 *Statoric currents* 57
Figure 5 *Rotoric currents* 57
Figure 6 *Statoric Flow* 58
Figure 7 *Rotoric flow* 58
Figure 8 *Statoric flow (α; β)* 58
Figure 9 *Electromagnetic torque* 59
Figure 10 *Rotation speed* 59
Figure 11 *Rotational speed* 59
Figure 12 *Electromagnetic torque* 59
Figure 13 *Statoric currents* 59
Figure 14 *Rotoric currents* 59
Figure 15 *Statoric Flow* 60
Figure 16 *Rotoric flow* 60
Figure 17 *Rotation speed* 60

Figure 18 *Electromagnetic torque* 60
Figure 19 *Rotational speed* 61
Figure 20 *Electromagnetic torque* 61
Figure 21 *Statoric currents* 61
Figure 22 *Rotoric currents* 61
Figure 23 *Statoric Flow* 61
Figure 24 *Rotoric flow* 61
Figure 25 *Statoric flow (α; β)* 62
Figure 26 *Rotation speed* 62
Figure 27 *Electromagnetic torque* 62

List of Tables

LIST OF TABLES

Page

CHAPTER II

Modeling of the doubly fed induction machine

Table 1 *Establishing the Expressions of Simple and Compound Tensions* 34

CHAPTER III

Direct Torque Control (DTC) of the doubly fed induction machine

Table 1 *Evolution of the flux and torque quantities as a function of the vector Vs applied in zone i* 46

Table 2 *Control strategy with a three-level hysteresis comparator (with non-zero voltage vectors)* 52

Table 3 *Control strategy with a three-level hysteresis comparator (with non-zero voltage vectors)* 52

Chapter IV

Direct Torque Control simulation

Table 1 *Variation in speed* 56

Table 2 *Load torque variation* 57

Abbreviations

Abbreviations

T_e T_{em}: Electromagnetic torque of the machine (N. m).
T_r: Resistant torque (N. m).
J: Inertia of rotating masses (Kg. $m2$).
f:viscous friction coefficient (Nms/rd).
I, i: Current(A).
I_{sd}: Stator current on the d axis (A).
I_{sq}: Stator current on axisq(A).
I_{rd}: Rotor currents on the d axis (A).
I_{rq}: Rotoric current on the q axis (A).
V_{sd}: Stator voltage on the d axis (V),
V_{rq}: Rotor tension on the d axis (V).
U_{ab}, U_{bc}, U_{ca}: the voltages composed from the outputs of the inverter (V).
V_{an}, V_{bn}, V_{cn}: the simple voltages of the phases of the load resulting from the compound voltages (V).
U_{dc}: DC voltage source of the inverter (V).
V_{abcM}: Tension of half arm A, B or C (V).
V_{abc}: Inverter output voltage A, B or C (V).
$V_{réf}$123: Reference voltage 1, 2 or 3 (sinusoidal)(V).
V_m: Amplitude of the reference voltage (V).
V_p: Triangular carrier (V)
$[V_{as}V_{bs}\ V_{cs}]^T$, $[V_{ar}\ V_{br}\ V_{cr}]^T$: Vectors of stator and rotor voltages (V).
$[I_{as}\ I_{bs}\ I_{cs}]^T$, $[I_{ar}\ I_{br}\ I_{cr}]T$: Vectors of stator and rotor currents (V).
$[\varphi_{as}\ \varphi_{bs}\ \varphi_{cs}]^T$, $[\varphi_{ar}\ \varphi_{br}\ \varphi_{cr}]^T$: Vectors of stator and rotor fluxes (V).
S_a, S_b, S_c: Represent the logic state of the voltage inverter switches
V_s: Voltage applied to the stator (V).
V_r: Voltage applied to the rotor (V).
V_i: Choice of voltage vector.
T_P: Carrier period (sec).
V_{pm}: Amplitude of the triangular carrier (V).
φ_{sd}: Stator flow on the d axis (Wb).
φ_{sa}: Stator flow on the α axis (Wb).
φ_{sq}: Stator flow on the q axis (Wb).
$\varphi_{s\beta}$: Stator flow on the β axis (Wb).
φ_{rd}: Rotor flow on the d axis (Wb).
$\varphi_{r\alpha}$: Rotor flow on the axis α(Wb).
φ_{rq}: Rotor flow on the q axis (Wb).
$\varphi_{r\beta}$: Rotor flux on the β axis (Wb).
$P_{network}$: Electrical power passing between the network and the DFIM (W).
P_m: Mechanical power supplied or received by the DFIM (W).
P_r: Electrical power supplied or received by the rotor of the DFIM (W).
P_s: Electrical power supplied or received by the DFIM stator (W).
$f_{réf}$: Frequency of the reference voltage (Hz).
f_p: Frequency of the triangular carrier (Hz).
f_s: Stator frequencies (Hz).
f_r: Rotor frequencies (Hz).
ω_s: Pulsation of stator currents (rad/sec).

$\omega = P\Omega$: Electrical pulsation of the rotor (rad. sec^{-1}).
ω_g: Sliding pulsation (rad/sec).
ω_{obs}: Pulsation of axis reference frame (d, q), (rad. sec^{-1}).
ω_n: $P\Omega$n: Nominal angular speed of the machine (rad/sec).
$\omega_r = d\theta r/dt$: Mechanical pulsation (rad/sec).
$\omega_s = d\theta s/dt$: Mechanical pulsation (rad/sec).
ω_n: Mechanical pulsation (rad/sec).
(Ω): Mechanical speed (Rad/sec).
(Ω′): Reference speed (Rad/sec).
Ω_s: Speed of the rotating field or synchronism speed (rad/s)
θ_s: Stator position (rad).
θ: Position between the stator axis as and the rotor axis ar (rad).
θ_r: Electrical rotor position (rad).
s: Index of the axes corresponding to the stator.
r: Index of the axes corresponding to the rotor.
a_s, b_s, c_s: Correspond to the three phases of the stator.
a_r, b_r, c_r: Correspond to the three phases of the rotor.
d: Direct axis index.
q: Quadrature axis index.
o: Index of the homopolar axis
m: Modulation indices.
R_s, R_r: Stator and rotor resistance (Ω).
L_s, L_r: Stator and rotor cyclic inductances (H).
M_s: Mutual inductance between stator phases (H).
M_r: Mutual inductance between rotor phases (H).
[M_{sr}]: Matrix of mutual inductances between the stator and rotor phases (H).
M: Mutual inductance between stator and rotor phases (H).
[L_s], [L_r]: Stator and rotor clean inductance matrices (H).
[R_s], [R_r]: Matrices of stator and rotor resistances (Ω).
[M_{ss}], [M_{rr}]: Stator − stator and rotor − rotor mutual inductance matrices (Ω).
$\dot{X} = dx/dt$: derived from the state vector.
X:State vector.
A: System state evolution matrix.
B: Order matrix.
U: Vector of the control system.
IP: Proportional integral regulator
$K_{p\Omega}$: Proportional gain of the IP speed regulator.
$K_{i\Omega}$: Integral gain of the IP speed regulator.
T_e: Sampling period.
s = (d/dt) : Laplace operator.
ξ:Damping constant.
(d, q): Longitudinal and quadrature axes of the Park reference frame.
(α, β): Longitudinal and quadrature axes of the Concordia benchmark.
[P(θ)]: Park matrix.
[P(θ)]: Inverse Park matrix.
g: Slip coefficient.
P:Number of pole pairs of the DFIM
γ: The angle between the two stator and rotor flux vectors.

Acronyms used:

DFIM: Double Fed Induction Machine
PWM: Pulse Width Modulation.
DTC: Direct Torque Control.
Cflx: Flux corrector.
Ccpl: Torque corrector.

General Introduction

General Introduction

Subsequently in the era of industrialization, researchers were confronted with the how to control electric machines at variable speeds, as electric drives increasingly require high performance, increased reliability, and reduced cost [1]

In the 19th century, this obstacle was solved with DC motors whose rotational speed could be changed from zero to maximum speed, and this by acting on the armature voltage while keeping the induction flow constant. However, the presence of the collector brush system penalizes them: these machines cannot be used either in the high-power field or in corrosive environments, and there is also the maintenance required by the collector [2]

These constraints have therefore oriented research in the field of variable speed towards alternating current machines, and more particularly towards asynchronous machines. These have many advantages: lower manufacturing costs, relatively simple construction, overload support, higher rotational speed and do not require permanent maintenance. The disadvantage of this category of machines lies in the complexity of their operation, as they behave like multi-variable, non-linear and strongly coupled systems, hence the difficulty of their control.

Thanks to technological developments in power electronics and microcomputing, the field of variable speed electric drives has experienced considerable growth in recent years, which has overcome the problems inherent in the control of reciprocating machines.

There is a new solution using the alternative machine operating in a rather particular mode, it is the "DFIM" doubly fed asynchronous machine. In fact, a special and significant effort is devoted to this machine because of the many advantages it offers, namely: accessibility to the stator and rotor, a wide range of speed variations, size compaction of the converters. Some studies make it a serious competitor to several electric machines, particularly the classic asynchronous cage machine. Yet at first glance, the scales seem to tip right away on the side of the squirrel cage machine, in fact, the asynchronous machine with wound rotor is larger (more copper), uses brushes and needs more converters for motor operation.

Several choices are used for the speed control of electric machines, and this control can be achieved in different ways and following different strategies. The first control that was introduced to the industry was the scalar control, which was widespread for its simplicity and low cost, and occupied a large part of industrial applications with variable speeds. However,

the demands for more efficient applications have opened the way for researchers to realize appropriate controls that meet industrial requirements. Vector control is currently a particularly interesting area of research, ranging from small power to high power drives. It is the modification of scalar control while maintaining its performance in transient regimes. The big difference between these two control strategies lies in the fact that for vector control, the machine parameters must be known quite precisely, the dynamics of the control become more and more efficient with a good parametric knowledge. But this change in tuning and the increase in dynamic performance come at a high price. This is the fact that has led other researchers to find orders that are just as efficient and less expensive. These efforts were rewarded by the introduction of Direct Torque Control (DTC), which was designed primarily to compete with its predecessor, which proved its worth but was not without its drawbacks. Thanks to current developments, a lot of research work aims to develop the performance of these two main methods. [3]

The objective of this work is to realize the strategy of a direct torque control of an asynchronous motor with dual feeding. To this end, the work plan was chosen, consisting of three chapters organized as follows:

The first chapter, presents a theoretical study on the asynchronous doubly fed machine (DFIM) concerning its operating principle and its disadvantages and advantages.

The second chapter is devoted to the mathematical model of the asynchronous dual-feed machine based on simplifying assumptions in the various benchmarks and the modeling of the DFIM power system. we used MATLAB/SIMULINK as a means of simulating our system.

The third chapter shows the feasibility of applying the DTC control technique on a double-feed machine. This chapter has made it possible to study Principle of DTC control and Operation of a three-phase voltage inverter and Control of stator flow and electromagnetic torque and Choice of voltage vector and Estimators and Elaboration of the control vector and Elaboration of the control table, the behavior of the direct control of the torque of the asynchronous double-fed machine powered by two two-stage voltage inverters.

Finally, the fourth chapter will focus on the simulation of the direct torque control of the asynchronous dual-feed machine under the Matlab/Simulink environment.

Chapter I

State of the art of the doubly fed induction machine (DFIM)

I.1. Introduction

The doubly fed induction machine (DFIM), also known as the asynchronous wound rotor machine or the doubly fed induction machine, is commonly used for the production of electrical power driven by wind and hydraulic turbines at variable speed and for powerful drives such as railway traction and marine propulsion. It belongs to the category of conventional asynchronous machines that represent good robustness and low maintenance cost due to the presence of separate three-phase stator and rotor windings, each powered by a different power source. This particular structure allows them to offer better control of speed and power, as well as increased energy efficiency.

In this study, we will take a closer look at the structure, operation, and benefits of doubly fed induction machine. We'll start with a brief description of their basic structure, going over the main components that make them up. We will then discuss how these machines work, highlighting the main factors that influence their performance. Finally, we will look at the benefits of doubly fed technology, highlighting the reasons why it is increasingly being used in industrial applications.

I.2. Description of the doubly fed induction machine

The Doubly Fed Induction Machine (DFIM), also known as the wound rotor induction generator, is a type of asynchronous electric motor with a unique design that allows for bidirectional energy flow. It's often used in applications where variable speed and high efficiency are crucial, such as wind turbines, pumps, and industrial processes. [1]

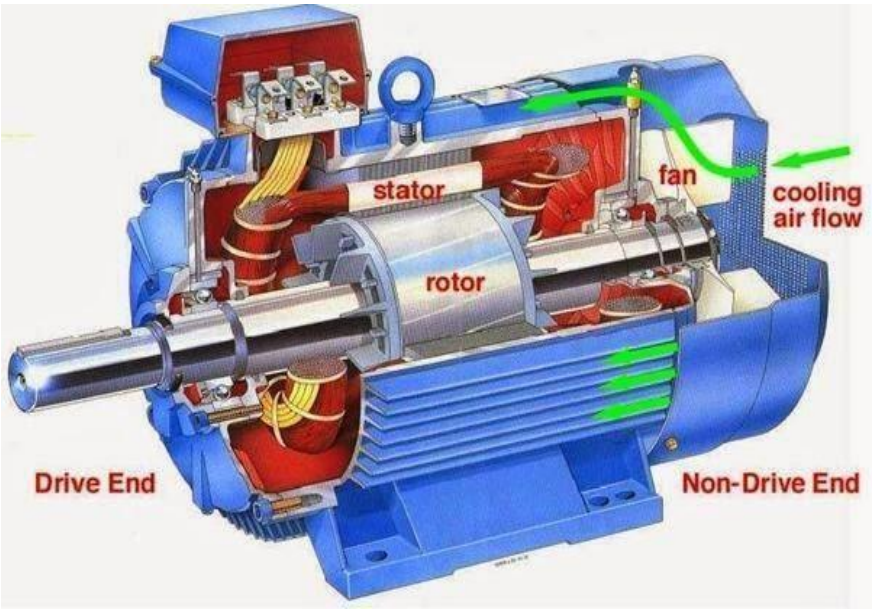

Figure I.1: Construction of Induction Motor[2].

Here's a breakdown of its key components and operation:

I.2.1. Stator

The stator is the fixed part of the motor. A cast iron or light alloy frame surrounds a ring of thin laminations (around 0.5 mm thick) made of silicon steel. The stator windings, which generate the spinning field (three windings for a three-phase motor), are held in place by slots in the laminations. A number of coils make up each winding. The number of pair poles in the motor and, therefore, its rotational speed is determined by the way these coils are connected to one another.

The structure of the stator is illustrated in both figures I.2 and I.3[3].

Figure I.2: An overview of the stator structure [3]

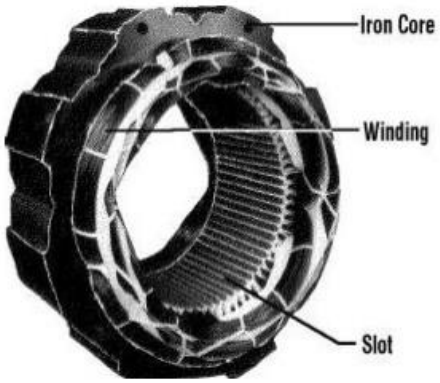

Figure I.3: Stator composition[3]

I.2.2. Rotor

The rotor is the rotating part of the machine. Unlike a standard induction motor where the rotor consists of short-circuited bars (squirrel-cage rotor), the DFIM's rotor has its own set of three-phase windings. These windings are connected to the external circuit via slip rings and brushes, allowing for external control of the rotor currents.

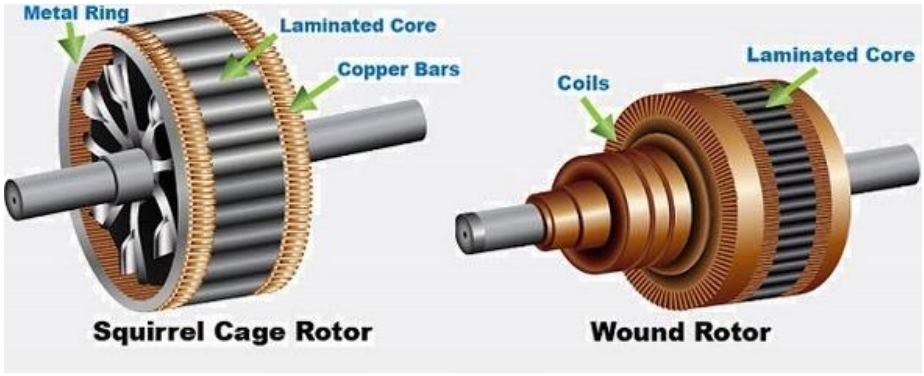

Figure I.4: Squirrel Cage Rotor Vs Wound Rotor[2]

I.2.3. Slip Rings and Brushes

These components enable electrical connections to the rotor windings. Unlike squirrel-cage rotors, where there are no external connections to the rotor, slip rings and brushes facilitate the transfer of electrical power and control signals to and from the rotor windings[4].

I.2.4. Power Electronics

The DFIM utilizes power electronic converters to control the flow of electrical energy between the stator and rotor windings. Typically, there are two sets of power converters—one connected to the rotor circuit (referred to as the rotor-side converter) and another connected to the stator circuit (referred to as the grid-side converter). These converters enable variable frequency and variable voltage operation, allowing for precise control of the machine's speed and torque.

I.2.5. Variable Speed Operation

One of the significant advantages of the DFIM is its ability to operate at variable speeds. By controlling the frequency and amplitude of the currents in the rotor windings, the speed of the machine can be adjusted independently of the grid frequency. This feature is particularly beneficial in applications like wind turbines, where wind speeds vary, and optimal energy capture requires variable speed operation.

I.2.6. Bidirectional Power Flow

Another key advantage of the DFIM is its ability to both generate and consume electrical power. In wind turbine applications, for example, the DFIM can act as a generator, converting mechanical energy from the wind into electrical energy. Conversely, in certain scenarios, such as during startup or high-speed operation, the DFIM can consume electrical energy to provide additional torque or control[5].

Overall, the Doubly Fed Induction Machine offers a flexible and efficient solution for applications requiring variable speed operation and bidirectional power flow. Its unique design and control capabilities make it well-suited for renewable energy generation, industrial processes, and other applications where precise control and high efficiency are essential.

I.3. Classification of the doubly fed induction machine

Several DFIM machines are developed and improved, these machines can be classified as following [6], [7-8]:

I.3.1. Single doubly fed machine

The Doubly Fed Induction Machine (DFIM.s) is an asynchronous wound rotor machine occupied by a brush-ring system (Single Doubly Fed Induction Machine). (Figure I.5)

illustrates the schematic diagram of the latter, such that the stator is supplied directly from the grid, as well as the rotor is supplied by means of an AC-AC converter in such a way that the slippage of the machine can be controlled. It should be noted that the converter shown in the figure can be composed of a rectifier and an inverter (indirect conversion) or can be a cyclo-converter (direct conversion) [2-5].

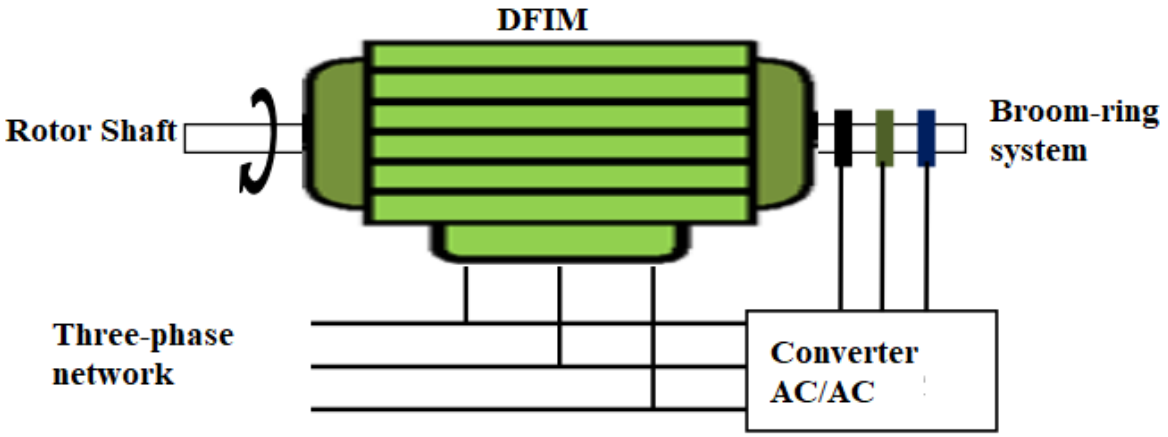

Figure I.5: Schematic Diagram of Single doubly fed machine [3]

I.3.2. Cascaded Doubly Fed Induction Machine

This machine consists of two DFIMs whose rotors are electrically and mechanically coupled. Figure (I.6) shows the schematic diagram of two asynchronous wound rotor machines for a doubly -feed system. The stator windings are connected to two three-phase voltage sources [3].

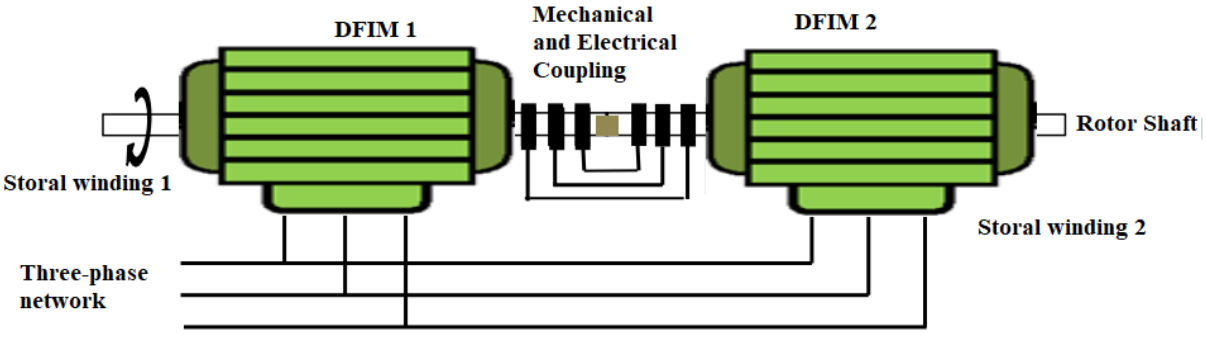

Figure I.6: Schematic Diagram of Cascaded Doubly Fed Induction Machine[3]

I.3.3. Single Frame Cascaded Doubly Fed Induction Machine

The Single Frame Cascaded Doubly Fed Induction Machine consists of two mechanically connected asynchronous cage induction machines. Figure (I.7) shows the schematic diagram, such that the stator of one of the two machines is connected directly to the grid while the other is connected to it via an AC-AC converter [3].

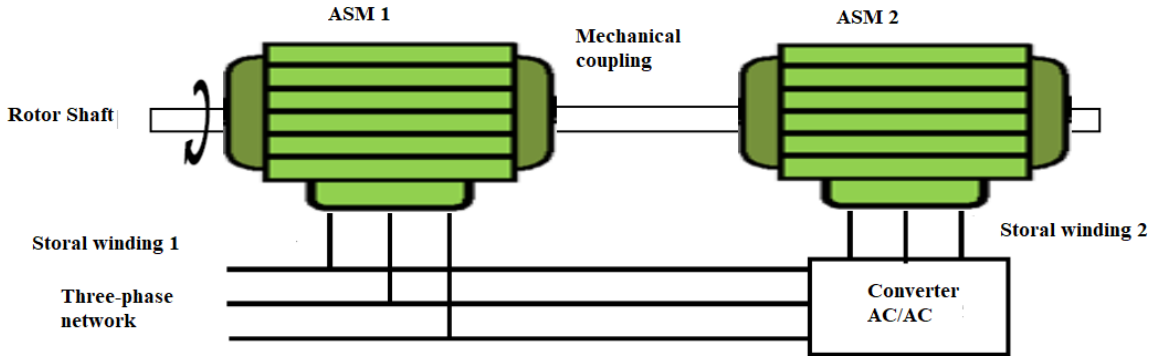

Figure I.7: Schematic Diagram of Single Frame Cascaded Doubly Fed Induction Machine[3]

I.3.4. Doubly Fed Machine Without Collector

This machine consists of two extended windings in a single stator. One of the two windings is powered directly from the mains and the other by an AC/AC converter as shown in Figure (I.8), This type of machine consists of two stator windings having different numbers of pole pairs; as well as that of the rotor must be the sum of these two numbers of pole pairs [6].

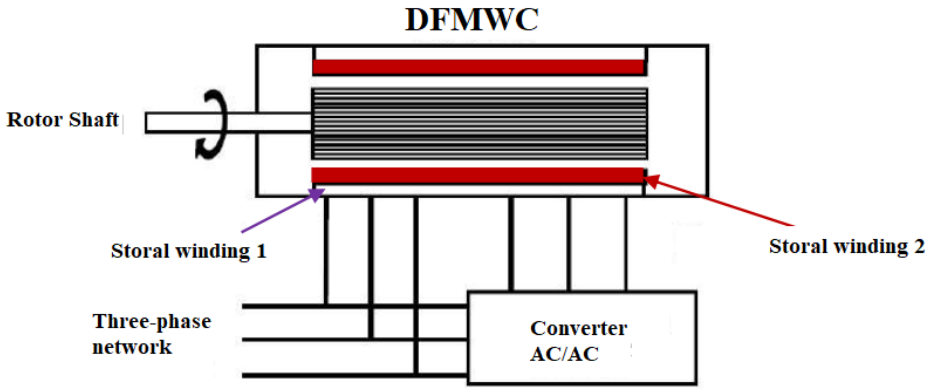

Figure I.8: Schematic Diagram of Doubly Fed machine without collector[1]

I.3.5. Brushless Doubly Fed Induction Machine

The idea of the brushless doubly fed machine BDFIM first developed by Steinmetz at the end of the 19th century. The assembly diagram of such a system is shown in Figure (I.9) where two wound rotor machines have been wedged on the same axis. The static windings of the two machines are connected to the network, while the rotor windings are interconnected with each other and therefore the bushings are de facto eliminated. The sliding power of the first machine is therefore used to excite the second machine. This elegant concept has long been in the perspective of designers as an effective solution for large power applications [7].

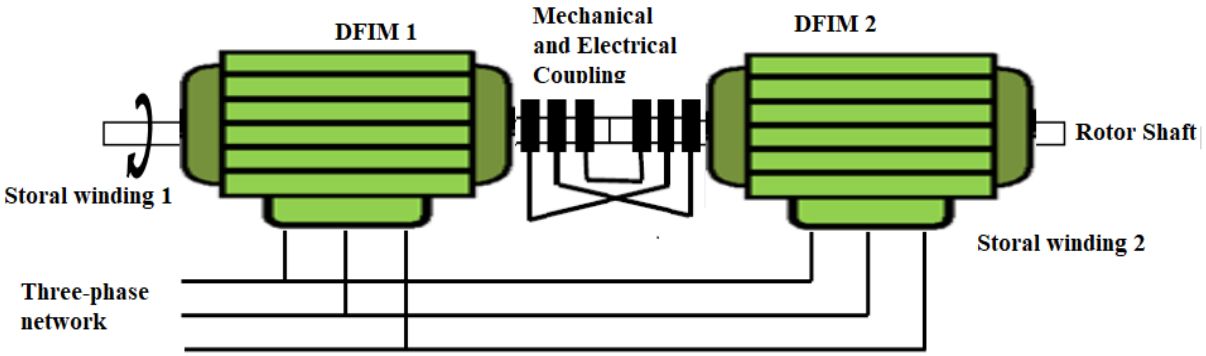

Figure I.9: Schematic Diagram of Brushless Doubly Fed Induction Machine[3]

According to this illustrated classification, it can be seen that the single doubly fed machine, represents an established construction compared to other types of machines.

I.4. Operating principle of DFIM

Virtually all electrical motors use magnetic field rotation to spin their rotors. A three-phase AC induction motor is the only type where the rotating magnetic field is created naturally in the stator because of the nature of the supply. DC motors depend either on mechanical or electronic commutation to create rotating magnetic fields. A single-phase AC induction motor depends on extra electrical components to produce this rotating magnetic field. Two sets of electromagnets are formed inside any motor. In an AC induction motor, one set of electromagnets is formed in the stator because of the AC supply connected to the stator windings. The alternating nature of the supply voltage induces an Electromagnetic Force (EMF) in the rotor (just like the voltage is induced in the transformer secondary) as per Lenz's law, thus generating another set of electromagnets, hence the name-induction motor Interaction between the magnetic field of these electromagnets generates twisting force, or torque. As result, the motor rotates in the direction of the resultant torque. [7]

I.5. Operating modes of DFIM

Only the mode of operation with the stator directly connected to the grid and the rotor powered by an inverter concerns us in this study.

Like the classic asynchronous machine, the DFIM can be operated as a motor or generator, but the big difference is that for the DFIM, it is no longer the rotational speed that dictates the motor or generator mode of operation.

Indeed, a cage machine must run below its synchronization speed to be in engine mode and above it in order to be in generator. Here, it is the control of the rotor voltages that allows the magnetic field inside the machine to be managed, thus offering the possibility of operating

in hyper or hypo synchronization both in motor mode and in generator mode. We will present these different modes of operation in turn.

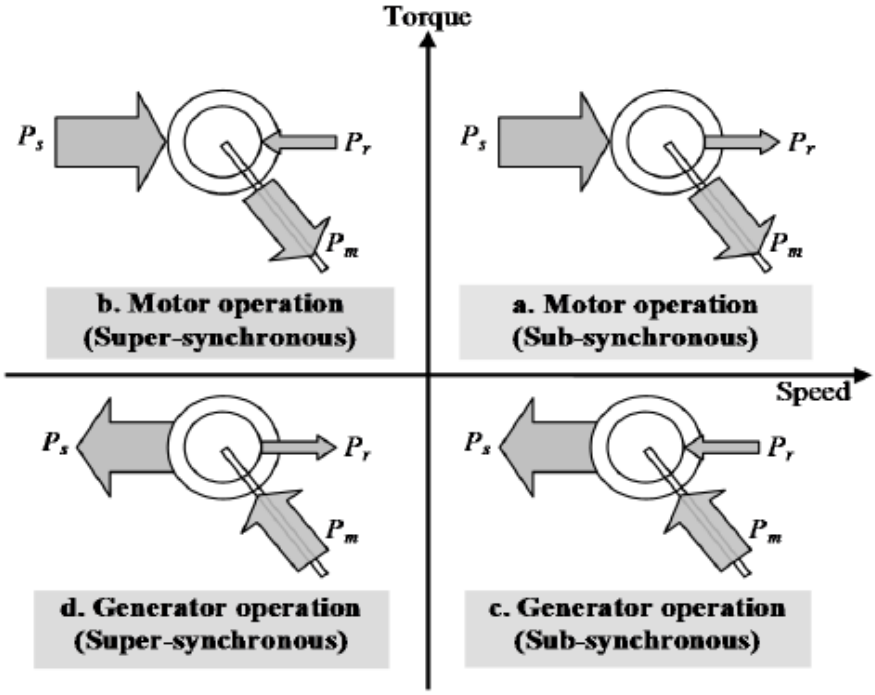

Figure I.10: Operational modes characteristic of the DFIM[8].

I.5.1. Motoring at Sub-synchronous Speed

In this mode, the DFIM operates as a motor, with electrical power being fed to the stator and mechanical power being produced at the shaft. [9]

The rotor speed (ω_r) is less than the synchronous speed (ω_s) of the stator magnetic field.

During this operation, the DFIM consumes reactive power from the grid.

This mode is useful for applications requiring variable speed operation, such as wind turbine generators and electric vehicles accelerating.

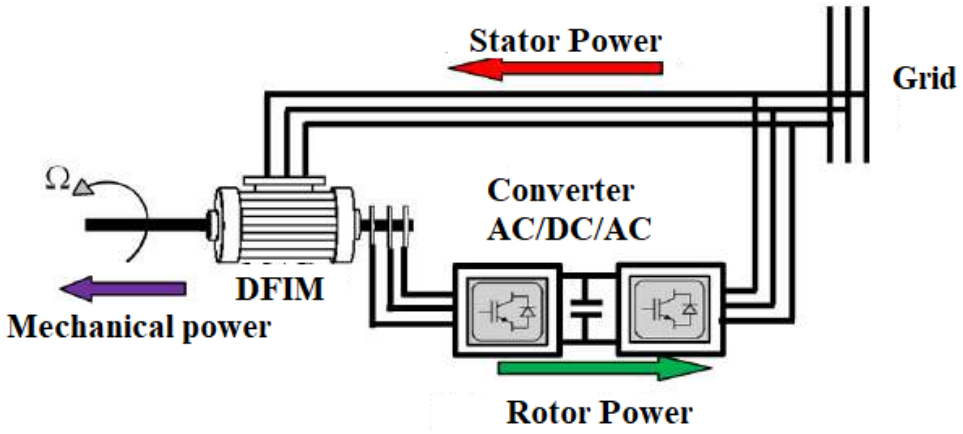

Figure I.11: Operation in hypo-synchronous motor mode[10]

I.5.2. Motoring at Super-synchronous Speed

Here, the DFIM also operates as a motor, but with the rotor speed (ω_r) exceeding the synchronous speed (ω_s) of the stator magnetic field. [9]

In this mode, the DFIM consumes electrical power from the grid and injects reactive power back into the grid.

This mode can be used for regenerative braking applications, where the kinetic energy of the motor is converted back into electrical energy and fed back to the grid.

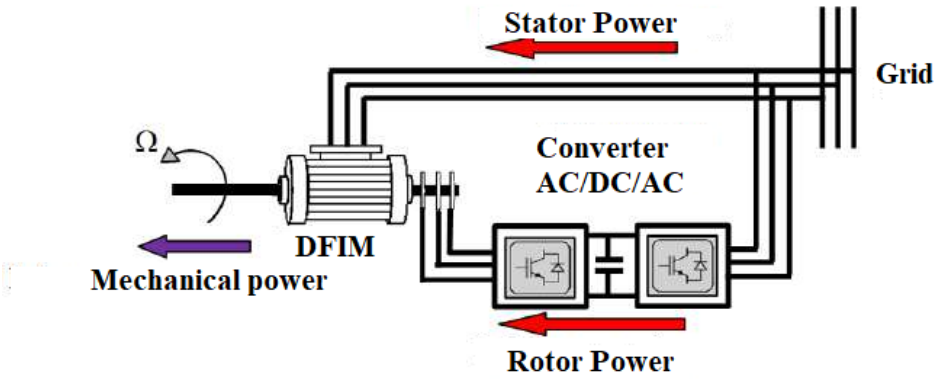

Figure I.12: Operation in hyper-synchronous motor mode[10]

I.5.3. Generating at Sub-synchronous Speed

In this mode, the DFIM acts as a generator, converting mechanical power input at the shaft into electrical power. [10]

The rotor speed (ω_r) is less than the synchronous speed (ω_s) of the stator magnetic field.

During generation, the DFIM injects both real and reactive power into the grid.

This operating mode is commonly used in wind turbine generators, where the wind turbine shaft provides the mechanical power input.

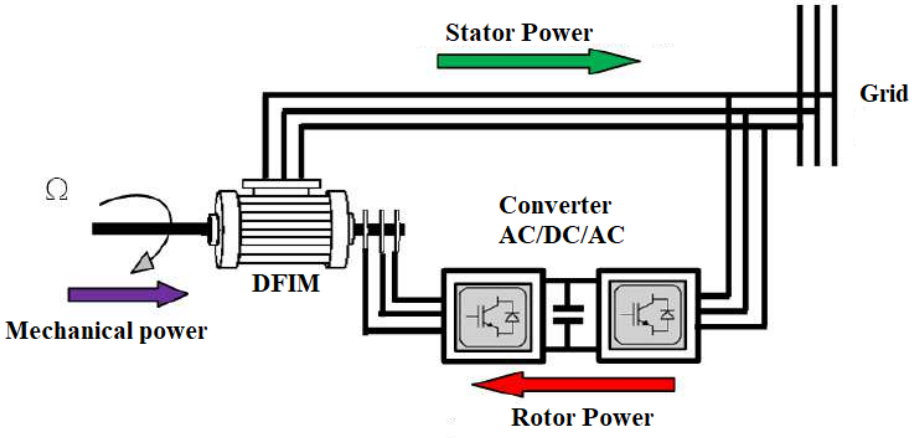

Figure I.13: Operation in hypo-synchronous generator mode[10]

I.5.4. Generating at Super-synchronous Speed

This mode is similar to generation at subsynchronous speed, but with the rotor speed (ω_r) exceeding the synchronous speed (ω_s) of the stator magnetic field. [9]

The DFIM injects both real and reactive power into the grid.

This mode is less common than subsynchronous generation but can occur in some wind turbine operating conditions. By controlling the injected rotor voltage and current, the DFIM's operating mode can be adjusted to meet the specific application requirements. This flexibility makes DFIMs valuable components in various industrial applications.

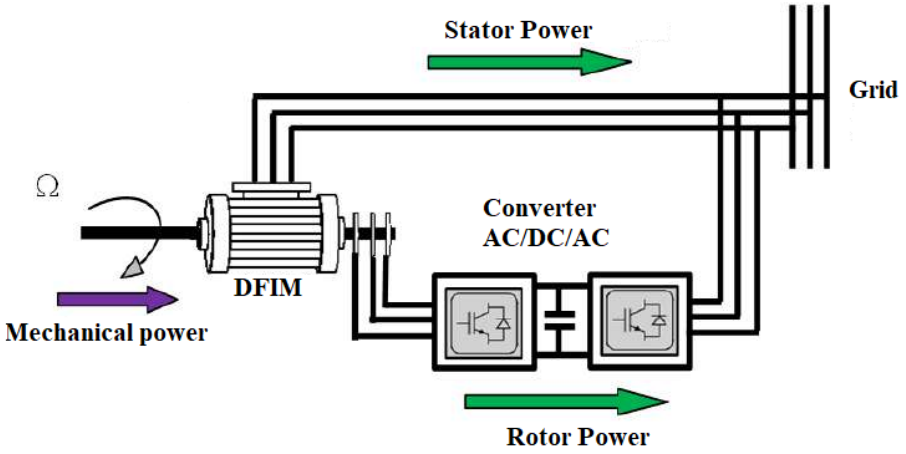

Figure I.14: Operation in hyper-synchronous generator mode[10]

I.6. Operation in hyper-synchronous generator mode

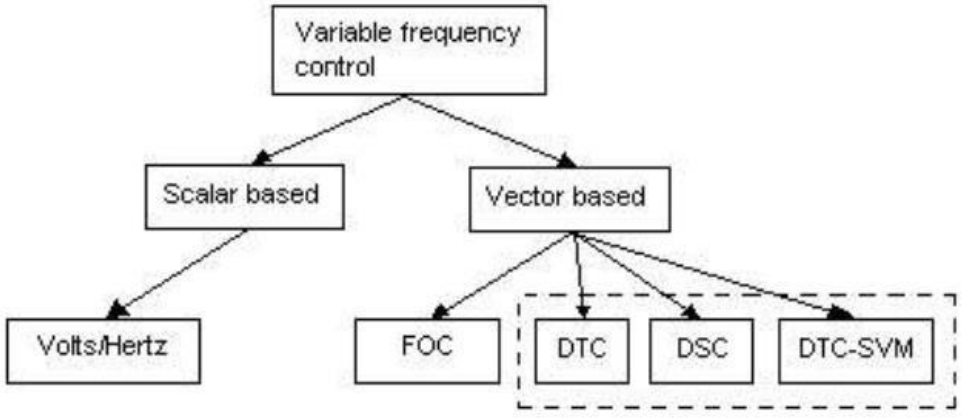

Figure I.15: Diagram of the different control strategies of an IM [10]

The diagram shown in the fig. I.15 illustrates the different control strategies existing of an induction motor [11]. These strategies can be classified into three main classes:

- Variable frequency drive
- Nonlinear control techniques
- Sensorless techniques

I.6.1. Variable frequency drive

We have two main variable frequency drive types, which are[12]:

I.6.1.1. Scalar control

Known also by "Volt/Hertz control", this technique is used to control the speed of the induction motors and all its techniques are mainly implemented through direct measurement of the machine parameters. The concept of V/f method is to keep the ratio of the stator voltage to frequency constant to maintain constant maximum available torque.

I.6.1.2. Vector control

a. Field oriented control

Field oriented control method, known popularly as vector control is widely used in modern industrial systems. In the opposite of the scalar control, the development of FOC control scheme is based on the dynamic model of the IM which make it valid for both steady and transient states.

The field oriented control method of the motor is realized for current components in d-q rotating coordinate system.

In the field oriented control system, a stator current d-component adjusts the rotor flux in the motor, while the combination of d and q-components adjusts the motor torque. By applying the decoupling block in the particular d and q control parts the control of flux and torque can be done independently.

b. The direct torque control DTC

The direct torque control is a robust control method which is based first in estimating the machine stator flux and electric torque in the stationary reference frame from terminal measurements.

The estimated stator flux and electric torque are then controlled directly by comparing them with their respective demanded values using hysteresis comparators.

The outputs of the two comparators are then used as input signals of an optimal switching table [11].

I.6.2. Nonlinear control techniques

There are two types of nonlinear control techniques:

I.6.2.1. Feed-back linearization

By employing state feedback, nonlinear dynamics are transformed into a linear form by feedback linearization. For input-output linearized and decoupled multiple input multiple output systems, control design and stabilization may be made simpler by using a conventional linear control. This approach does have certain drawbacks, though. For instance, it only

applies to nonlinear systems having a precise mathematical description; it is not relevant to all other nonlinear systems. It is not possible to ensure the resilience of the system in the presence of parameter uncertainty.

I.6.2.2. Sliding mode control

The sliding mode control (SMC) is a particular type of variable structure control (VSC). Its first concepts appeared in the Soviet Union in 1950s and were later on developed by Emelyanov in 1960s. This method is designed to drive and then to constrain the system state to lie within a neighborhood of the switching surface. Its main features are the dynamics behavior of the system which may be tailored at a particular choice of switching function. This approach is independent of the object parameters which make the closed loop response becomes totally insensitive to a particular class of uncertainty in the system, which provides a very strong and inherent robustness to the resulting controllers. [12]

I.6.3. Sensorless control techniques

In electric drives, measuring speed and flux is a crucial first step in control design, irrespective of the kind of control method employed. Control methods cannot be implemented until all of the state vector's components are understood. However, using sensors is harmful for them because to their high cost, fragility, and decreased dependability. Aside from the fact that sensors need to be maintained on a regular basis, there are certain applications where installing sensors is improper because of environmental and physical limitations. A similar circumstance occurs when a sensor malfunctions.

Thus, a plan of action was put forward to get around these obstacles and constraints. The idea is to use software sensors in place of physical sensors. In the realm of automation, sensorless control theory is well-known and plays a significant role. Observers or estimators are the names given to the software sensors. This sensorless control for electrical devices aims to calculate the location and mechanical speed and torque, or flux vector. In the last 10 years, industry applications for speed sensorless AC drive control have grown significantly since it may save costs and eliminate the hassle of installing mechanical sensors.

I.7. Areas of application of DFIM

Here are some areas of application for DFIM[13]:

- **Wind Power Generation:** DFIMs are commonly used in wind turbines. They allow for variable speed operation, which is beneficial for extracting maximum power from varying wind speeds. The ability to control both the rotor and stator currents independently enables efficient power generation and grid integration.

- **Marine Propulsion:** DFIMs can be used in marine propulsion systems, such as ship propulsion and thrusters. They offer efficient variable speed control, which is useful for maneuverability and energy savings in marine vessels.
- **Industrial Applications: DFIMs** find applications in various industrial processes requiring variable speed control, such as pumps, compressors, fans, and conveyors. Their ability to efficiently handle variable loads and adjust speed according to process requirements makes them suitable for industrial automation.
- **Electric Vehicles (EVs):** DFIMs can be employed in electric vehicle propulsion systems, including electric cars, buses, and trains. Their variable speed capabilities allow for better control over acceleration and energy efficiency, contributing to extended battery life and increased driving range.
- **Renewable Energy Integration:** DFIMs can be used in other renewable energy systems besides wind, such as small hydroelectric power plants or tidal energy converters. Their ability to efficiently convert variable mechanical power into electrical power, along with grid-friendly characteristics, makes them suitable for integrating renewable energy sources into the grid.
- **Microgrids and Energy Storage Systems:** DFIMs can play a role in microgrid applications, where distributed energy resources need to be integrated and managed efficiently. They can also be coupled with energy storage systems to provide grid stabilization services and support renewable energy integration.
- **Smart Grids and Power Quality Improvement:** In smart grid applications, DFIMs can be utilized for power factor correction, voltage regulation, and reactive power compensation. Their controllability and grid-friendly features make them valuable assets for enhancing power quality and grid stability.
- **Research and Development:** DFIMs are also used in research and development activities related to motor control, power electronics, and renewable energy systems. They serve as testbeds for studying advanced control strategies, fault-tolerant operation, and grid integration techniques.

I.8. Advantages and disadvantages of DFIM

I.8.1. Advantages of DFIM

The doubly fed inductions machines (DFIM) are preferred for many industrial and renewable energy applications due to their unique properties. Some of the key benefits of DFIMs include[6]:

- Improved energy efficiency: DFIMs have higher levels of efficiency compared to other types of electrical machines, especially at partial loads. This is due to the fact that DFIMs have a smaller rotor circuit than the stator circuit, which reduces copper losses and wasted energy as heat.
- Variable speed operation: DFIMs can operate at variable speeds, which is an essential feature for renewable energy applications such as wind turbines. DFIMs allow the wind turbine to operate at varying wind speeds while maintaining optimal energy production.
- Cost-effectiveness: DFIMs are generally less expensive than other types of electrical machines, such as permanent magnet machines. DFIMs have a simpler structure and do not require expensive scarce materials, making them a cost-effective option for many applications.
- Regenerative Braking: DFIMs can operate in both motor and generator mode, which means they can be used for regenerative braking. During braking, the DFIM can convert the kinetic energy of the rotating load into electrical energy, which can be fed back into the grid or stored in a battery. This improves fuel efficiency and reduces the amount of heat generated during braking.

In summary, DFIMs offer several advantages over other types of electric machines, such as improved energy efficiency, variable speed operation, cost-effectiveness, regenerative braking, and high torque density. These advantages make DFIMs an ideal choice for many industrial and renewable energy applications.

I.8.2. Disadvantages of DFIM

While the doubly fed induction machine (DFIM) have many advantages, they also have some disadvantages, including[6]:

- Requires a frequency converter: DFIMs require a frequency converter to operate in variable mode, which can add additional costs and increase the complexity of the system.
- Need for regular maintenance: DFIMs require regular maintenance to ensure they function properly.
- Requires a sophisticated control system: DFIMs require a sophisticated control system to function optimally. The control system must be able to monitor and control the voltage, current, and frequency of the machine to ensure optimal power production.

I.9. Conclusion

In this chapter we have presented a general overview about the doubly fed induction machine (DFIM) and their application has been given as well as the different types of operation. The principle and operating regimes of the latter were also presented. DFIM has a character that allows it to occupy a wide field of application, both in variable speed drives (motor operation) and in variable speed and constant frequency applications (generator operation).

To make good use of the doubly fed induction machine in such an application area, modeling and vector control are required. The subject of the next chapter is devoted to the modeling of the doubly fed induction motor (DFIM). The next chapter will focus on DFIM modelling.

.

Chapter II

Modeling of the doubly fed induction machine

II.1. Introduction

The literature attests to the great interest given today to the doubly fed induction machine for various applications: as a generator for renewable energies or as an engine for certain industrial applications such as rolling, railway traction or maritime propulsion.

In this chapter, we are interested in modeling the Asynchronous Doubly Fed Induction Machine. Different modelling methods can be considered. Some of them are more appropriate to describe a particular phenomenon with the best compromise between accuracy and computation time and also simulation.

In the literature, we find three main approaches to modeling electrical machines:

- **Finite element modeling**

This type of modeling is the most accurate. These methods, which are particularly well suited to complex geometries, provide information on the evolution of fields at any point in the magnetic circuit. However, the computational time required by this approach is significant.

- **Permeance network modeling**

Permeance network modeling is based on the division of a magnetic circuit into permeances. This technique offers many advantages: the computation time is lower than models based on the finite element method, coupling with electrical circuit equations is easy. The main difficulty of this method lies in the representation of the air gap of the machine. The modeling error is very sensitive to the model used for the air gap permeances.

- **Modeling by electrical circuits**

Electrical circuit modeling is constructed from the electrical equations of the machine. This modeling method, very simple to formulate, offers a good compromise between calculation time and accuracy. This type of approach is well suited to the development of control algorithms. Only the latter modelling method will be used in this work. It is also called "two-axis theory". It is mainly based on a change of reference system known as "three-phase-two-phase transformation".

II.2. Three-phase model of DFIM

II.2.1. Description

The Doubly Fed Induction Machine (DFIM) is, as the name suggests, a three-phase AC machine with two accessible three-phase windings, in which power can be supplied or extracted from the machine through these windings.

This type of machine requires a single alternative power source that can supply both sides of the machine and this is a main advantage especially in variable speed drive and generation areas, where the slip can be modified by means of the combination of power converters on the stator or rotor side or both. This depends mainly on the construction. [11]

II.2.2. Hypothèse

To simplify the study of the asynchronous machine, the following simplifying assumptions are considered:

- ✓ The perfect symmetry of both magnetic and electric machines.
- ✓ The magnetomotive forces created by each phase of the stator or rotor have a sinusoidal distribution.
- ✓ The effect of temperature variation on stator and rotor resistances is negligible.
- ✓ The skin effect is neglected.
- ✓ The air gap is constant.
- ✓ The non-saturated magnetic circuit and constant permeability.
- ✓ Negligible ferromagnetic losses.
- ✓ The asynchronous machine with a dual power supply shall be shown in the three-phase system in Figure (II.1).

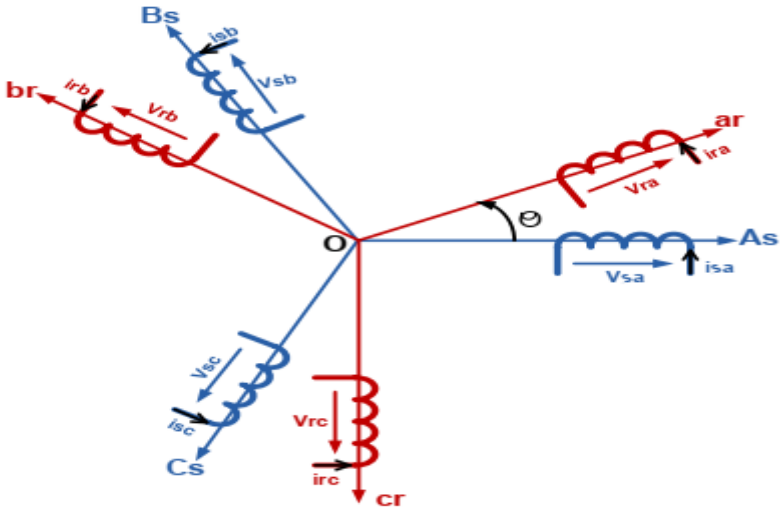

Figure II.1: Schematic representation of the DFIM[11]

II.2.3. Actual Electrical Equations of the Machine

The equations are written as follows [10]:

$$\begin{bmatrix} V_{SA} \\ V_{SB} \\ V_{SC} \end{bmatrix} = \begin{bmatrix} R_S & 0 & 0 \\ 0 & R_S & 0 \\ 0 & 0 & R_S \end{bmatrix} \begin{bmatrix} I_{SA} \\ I_{SB} \\ I_{SC} \end{bmatrix} + \frac{d}{dt} \begin{bmatrix} \emptyset_{SA} \\ \emptyset_{SB} \\ \emptyset_{SC} \end{bmatrix}, \begin{bmatrix} V_{RA} \\ V_{RB} \\ V_{RC} \end{bmatrix} = \begin{bmatrix} R_R & 0 & 0 \\ 0 & R_R & 0 \\ 0 & 0 & R_R \end{bmatrix} \begin{bmatrix} I_{RA} \\ I_{RB} \\ I_{RC} \end{bmatrix} + \frac{d}{dt} \begin{bmatrix} \emptyset_{RA} \\ \emptyset_{RB} \\ \emptyset_{RC} \end{bmatrix} \quad \text{(II.1)}$$

Or in the form of:

$$\begin{cases} [V_S] = [R_S][I_S] + \frac{d}{dt}[\emptyset_S] \\ [V_R] = [R_R][I_R] + \frac{d}{dt}[\emptyset_R] \end{cases} \quad \text{(II.2)}$$

II.2.4. Magnetic Equations

Magnetic equations are written as follows:

$$\begin{bmatrix} \emptyset_{SA} \\ \emptyset_{SB} \\ \emptyset_{SC} \end{bmatrix} = \begin{bmatrix} l_S & m_S & m_S \\ m_S & l_S & m_S \\ m_S & m_S & l_S \end{bmatrix} \begin{bmatrix} I_{SA} \\ I_{SB} \\ I_{SC} \end{bmatrix} + m_{SR} \begin{bmatrix} cos(\theta) & cos(\theta - 4\pi/3) & cos(\theta - 2\pi/3) \\ cos(\theta - 2\pi/3) & cos\,\theta & cos(\theta - 4\pi/3) \\ cos(\theta - 4\pi/3) & cos(\theta - 2\pi/3) & cos(\theta) \end{bmatrix} \begin{bmatrix} I_{Ra} \\ I_{Rb} \\ I_{Rc} \end{bmatrix} \quad \text{(II.3)}$$

$$\begin{bmatrix} \emptyset_{Ra} \\ \emptyset_{Rb} \\ \emptyset_{Rc} \end{bmatrix} = \begin{bmatrix} l_R & m_R & m_R \\ m_R & l_R & m_R \\ m_R & m_R & l_R \end{bmatrix} \begin{bmatrix} I_{Ra} \\ I_{Rb} \\ I_{Rc} \end{bmatrix} + m_{RS} \begin{bmatrix} cos(\theta) & cos(\theta - 2\pi/3) & cos(\theta - 4\pi/3) \\ cos(\theta - 4\pi/3) & cos\,\theta & cos(\theta - 2\pi/3) \\ cos(\theta - 2\pi/3) & cos(\theta - 4\pi/3) & cos(\theta) \end{bmatrix} \begin{bmatrix} I_{SA} \\ I_{SB} \\ I_{SC} \end{bmatrix} \quad \text{(II.4)}$$

Equations (II.3) and (II.4) can also be written as follows:

$$\begin{cases} [\emptyset_S] = [L_S][I_S] + m_{SR}[I_R] \\ [\emptyset_R] = [L_R][I_R] + m_{RS}[I_S] \end{cases} \quad \text{(II.5)}$$

Substituting equations (II.5) into (II.2) gives the following matrix expressions:

$$\begin{cases} [V_S] = [R_S][I_S] + [L_S]\frac{d}{dt}[I_S] + d/dt\,([M_{SR}][I_R]) \\ [V_R] = [R_R][I_R] + [L_R]\frac{d}{dt}[I_R] + d/dt\,([M_{SR}][I_S]) \end{cases} \quad \text{(II.6)}$$

The $[M_{RS}]$ matrix is likewise a circulating matrix, and we notice that it is the transposed matrix of the analogous matrix of the stator: $[M_{RS}] = [M_{SR}]^T$

II.3. Two-phase modelling of DFIM

II.3.1. Application of the Park Transformation

For the transition from three-phase to two-phase systems, the following matrix is used[14]:

$$\begin{bmatrix} X_d \\ X_q \\ X_0 \end{bmatrix} = \sqrt{\frac{2}{3}} \begin{bmatrix} cos(\theta) & cos(\theta - 2\pi/3) & cos(\theta - 4\pi/3) \\ -sin(\theta) & -sin(\theta - 2\pi/3) & -sin(\theta - 4\pi/3) \\ 1/\sqrt{2} & 1/\sqrt{2} & 1/\sqrt{2} \end{bmatrix} = \begin{bmatrix} X_a \\ X_b \\ X_c \end{bmatrix} \quad \text{(II.7)}$$

The real stator windings (A, B, C) and rotor windings (a, b, c) are transformed respectively into two fictitious stator windings and two fictitious rotor windings in the same two-phase reference frame (d, q, O) in order to simplify the equations. Let θr and θs be the electrical angles formed by the axes of the stator and rotor with the direct axis of Park's two-phase reference frame. [14]

Figure (II.2) illustrates the relative position of the different reference frames in space where θr and θs are naturally related to θ by the rigid relation:

$$\theta = \theta_s - \theta_r \quad \text{(II.8)}$$

This allows you to write:

$$\frac{d\theta}{dt} = \frac{d\theta_s}{dt} - \frac{d\theta_r}{dt} \quad \text{(II.9)}$$

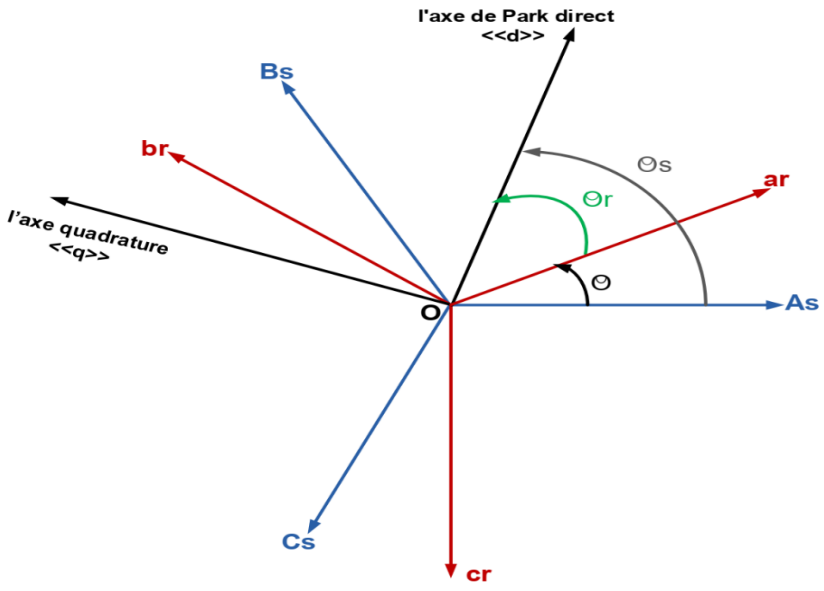

Figure II.2: Spatial position of the different reference frames[14]

The different quantities after applying the transformation to the stator are expressed by:

$$\begin{bmatrix} V_{Sd} \\ V_{Sq} \\ V_0 \end{bmatrix} = [P(\theta_s)] = \begin{bmatrix} V_{SA} \\ V_{SB} \\ V_{SC} \end{bmatrix}, \begin{bmatrix} V_{Sd} \\ V_{Sq} \\ V_0 \end{bmatrix} = [P(\theta_s)] = \begin{bmatrix} I_{SA} \\ I_{SB} \\ I_{SC} \end{bmatrix}, \begin{bmatrix} \emptyset_{Sd} \\ \emptyset_{Sq} \\ \emptyset_0 \end{bmatrix} = [P(\theta_s)] = \begin{bmatrix} \emptyset_{SA} \\ \emptyset_{SB} \\ \emptyset_{SC} \end{bmatrix} \quad \text{(II.10)}$$

And to the rotor by:

$$\begin{bmatrix} V_{Rd} \\ V_{Rq} \\ V_0 \end{bmatrix} = [P(\theta_R)] = \begin{bmatrix} V_{Ra} \\ V_{Rb} \\ V_{Rc} \end{bmatrix}, \begin{bmatrix} I_{Rd} \\ I_{Rq} \\ I_0 \end{bmatrix} = [P(\theta_R)]. \begin{bmatrix} I_{Ra} \\ I_{Rb} \\ I_{Rc} \end{bmatrix}, \begin{bmatrix} \emptyset_{Rd} \\ \emptyset_{Rq} \\ \emptyset_0 \end{bmatrix} = [P(\theta_R)]. \begin{bmatrix} \emptyset_{Ra} \\ \emptyset_{Rb} \\ \emptyset_{Rc} \end{bmatrix} \quad \text{(II.11)}$$

The mathematical model in Park's frame of reference:

II.3.1.1. Electrical equations:

Recall the expressions of the stator voltages in the three-phase reference frame given by[9]:

$$[V_S] = [R_S].[I_S] + \frac{d}{dt}[\emptyset_s] \quad \text{(II.12)}$$

After applying the Park transform, we get:

$$[P(\theta_s)]^{-1}[V_{sdq0}] = [R_S][P(\theta_s)]^{-1}.[I_{sdq0}] + \frac{d}{dt}\{[P(\theta_s)]^{-1}.[\emptyset_{sdq0}]\} \quad \text{(II.13)}$$

This gives by multiplying each of the members of the equation P(s) by the matrix equation of the voltages for the reference frame (d, q, O):

$$[V_{sdq0}] = [R_S][I_{sdq0}] + [P(\theta_s)].\frac{d}{dt}\{[P(\theta_s)]^{-1}\}.[\emptyset_{sdq0}] + \frac{d}{dt}\{[\emptyset_{sdq0}]\} \quad \text{(II.14)}$$

In addition, it is shown that:

$$[P(\theta_s)].\frac{d}{dt}\{[P(\theta_s)]^{-1}\} = \begin{bmatrix} 0 & -1 & 0 \\ 1 & 0 & 0 \\ 0 & 0 & 0 \end{bmatrix} \quad \text{(II.15)}$$

Where from:

$$\begin{cases} V_{Sd} = R_S I_{Sd} + \dfrac{d\emptyset_{Sd}}{dt} - \dfrac{d\theta_S}{dt}\emptyset_{Sq} \\ V_{Sq} = R_S I_{Sq} + \dfrac{d\emptyset_{Sq}}{dt} + \dfrac{d\theta_S}{dt}\emptyset_{Sd} \\ V_0 = R_S I_{S0} + \dfrac{d\emptyset_{S0}}{dt} = 0 \end{cases} \quad \text{(II.16)}$$

Similarly, for the rotor:

$$[V_{Rdq0}] = [R_R][I_{Rdq0}] + [P(\theta_R)].\frac{d}{dt}\{[P(\theta_R)]^{-1}\}.[\emptyset_{Rdq0}] + \frac{d}{dt}\{[\emptyset_{Rdq0}]\} \quad \text{(II.17)}$$

So we can write:

$$\begin{cases} V_{Rd} = R_R I_{Rd} + \dfrac{d\emptyset_{Rd}}{dt} - \dfrac{d\theta_R}{dt}\emptyset_{Rq} \\ V_{Rq} = R_R I_{Rq} + \dfrac{d\emptyset_{Rq}}{dt} + \dfrac{d\theta_R}{dt}\emptyset_{Rd} \\ V_0 = R_R I_{R0} + \dfrac{d\emptyset_{R0}}{dt} = 0 \end{cases} \quad \text{(II.18)}$$

II.3.1.2. Magnetic equations

Recall the expressions for the stator and rotor fluxes in the three-phase frame of reference given by the following relations [1]:

$$[\emptyset_S] = [L_S].[I_S] + [M_{SR}].[I_R] \quad \text{(II.19)}$$

$$[\emptyset_R] = [L_R].[I_R] + [M_{RS}].[I_S] \quad \text{(II.20)}$$

After applying Park's transformation, we get:

$$[P(\theta_S)]^{-1}.[\emptyset_{Sdq0}] = [L_S][P(\theta_S)]^{-1}[I_{Sdq0}] + [M_{SR}][P(\theta_S)]^{-1}[I_{Rdq0}] \quad \text{(II.21)}$$

$$[P(\theta_R)]^{-1}.[\emptyset_{Rdq0}] = [L_R][P(\theta_R)]^{-1}[I_{Rdq0}] + [M_{RS}][P(\theta_R)]^{-1}[I_{Sdq0}] \quad \text{(II.22)}$$

Finally, we obtain by developing:

$$\begin{bmatrix}\emptyset_{Sd}\\ \emptyset_{Sq}\\ \emptyset_{S0}\end{bmatrix} = \begin{bmatrix} l_s - m_s & 0 & 0 \\ 0 & l_s - m_s & 0 \\ 0 & 0 & l_s - m_s \end{bmatrix}\begin{bmatrix}I_{Sd}\\ I_{Sq}\\ I_{S0}\end{bmatrix} + \begin{bmatrix} (3/2)m_{SR} & 0 & 0 \\ 0 & (3/2)m_{SR} & 0 \\ 0 & 0 & (3/2)m_{SR} \end{bmatrix}\frac{d}{dt}\begin{bmatrix}I_{Rd}\\ I_{Rq}\\ I_{R0}\end{bmatrix} \quad \text{(II.23)}$$

$$\begin{bmatrix}\emptyset_{Rd}\\ \emptyset_{Rq}\\ \emptyset_{R0}\end{bmatrix} = \begin{bmatrix} l_R - m_R & 0 & 0 \\ 0 & l_R - m_R & 0 \\ 0 & 0 & l_R - m_R \end{bmatrix}\begin{bmatrix}I_{Rd}\\ I_{Rq}\\ I_{R0}\end{bmatrix} + \begin{bmatrix} (3/2)m_{SR} & 0 & 0 \\ 0 & (3/2)m_{SR} & 0 \\ 0 & 0 & (3/2)m_{SR} \end{bmatrix}\frac{d}{dt}\begin{bmatrix}I_{Sd}\\ I_{Sq}\\ I_{S0}\end{bmatrix} \quad \text{(II.24)}$$

Ask:

$L_S=l_S-m_S$ *:* Statoric cyclic inductance coefficient.

$L_R=l_R-m_R$ *:* Rotoric cyclic inductance coefficient.

$M_{SR}=3/2(m_{SR})$ *:* Cyclic mutual inductance coefficient between stator and rotor.

$L_{S0}=l_S-2.m_S$ *:* Statoric homopolar inductance coefficient.

$L_{R0}=l_R-2.m_R$ *:* Rotoric homopolar inductance coefficient.

The result is:

At the stator:

$$\begin{cases} \emptyset_{Sd} = L_S.I_{Sd} + M_{SR}.I_{Rd} \\ \emptyset_{Sq} = L_S.I_{Sq} + M_{SR}.I_{Rq} \\ \emptyset_{S0} = L_{S0}I_{S0} \end{cases} \quad \text{(II.25)}$$

At the rotor:

$$\begin{cases} \emptyset_{Rd} = L_R.I_{Rd} + M_{SR}.I_{Sd} \\ \emptyset_{Rq} = L_R.I_{Rq} + M_{SR}.I_{Sq} \\ \emptyset_{R0} = L_{R0}I_{R0} \end{cases} \quad \text{(II.26)}$$

The above equations can be transformed to determine the expressions of currents as functions of flows as follows [8]:

At the stator:

$$\begin{cases} I_{Sd} = \dfrac{1}{\sigma.L_S}.\emptyset_{Sd} - \dfrac{M_{SR}}{\sigma.L_S.L_R}.\emptyset_{Rd} \\ I_{Sq} = \dfrac{1}{\sigma.L_S}.\emptyset_{Sq} - \dfrac{M_{SR}}{\sigma.L_S.L_R}.\emptyset_{Rq} \\ I_{S0} = \dfrac{\emptyset_{S0}}{L_{S0}} \end{cases} \quad \text{(II.27)}$$

At the rotor:

$$\begin{cases} I_{Rd} = \dfrac{M_{SR}}{\sigma.L_S.L_R}.\emptyset_{Sd} + \dfrac{1}{\sigma.L_R}.\emptyset_{Rd} \\ I_{Rq} = \dfrac{M_{SR}}{\sigma.L_S.L_R}.\emptyset_{Sq} - \dfrac{1}{\sigma.L_R}.\emptyset_{Rq} \\ I_{R0} = \dfrac{\emptyset_{R0}}{L_{R0}} \end{cases} \quad \text{(II.28)}$$

We find that thanks to the substitution of fictitious two-phase windings for real three-phase windings, we arrive at a system in which:

- Flows now depend on only three parameters (L_S, L_R, M_{SR}).
- The inductance coefficients are independent of time, and therefore the dependence on the angle θ has disappeared.
- The matrices are diagonal, i.e. the quantities of the d and q axes are no longer coupled.

Figure (II.3) illustrates this lack of linkage:

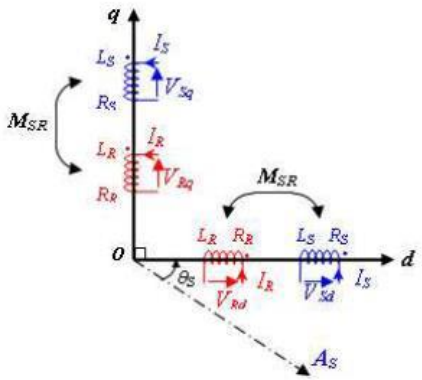

Figure II.3. Representation of d-axis and q-axis dummy windings[1]

Since the homopolar components of the different quantities are zero for equilibrium and non-degraded operating regimes, the Park transform reduces the order of the system.

II.3.1.3. The electromagnetic torque:

Electrical power can be put into the form of [7]:

$$P_{elec} = [V_s]^T.[I_S] = \left[V_{Sdq0}\right]^T.\left[I_{Sdq0}\right] = V_{Sd}.I_{Sd} + V_{Sq}.I_{Sq} + V_{SO}.I_{SO} \quad \text{(II.29)}$$

By replacing the direct and quadrature components with their expressions, and eliminating the term homopolar, we can write:

$$P_{elec} = \underbrace{\left[R_s.I_{Sd}^2 + R_s.I_{Sq}^2\right]}_{\text{Pertes joules}} + \underbrace{\left[\emptyset_{Sd}.I_{Sd} + \emptyset_{Sq}.I_{Sq}\right]}_{\text{Puissance réactive}} + \underbrace{\left[\theta_s\left(\emptyset_{Sd}.I_{Sq} - \emptyset_{Sq}.I_{Sd}\right)\right]}_{\text{Puissance électromagnétique}} \quad \text{(II.30)}$$

The expression of the electromagnetic torque can be determined by the following relationship:

$$T_{em} = P_{em}/\Omega_S \text{ and knowing that } \frac{d\theta_s}{dt} = \omega_s.p\Omega_S \quad \text{(II.31)}$$

So, we can write the expression of the couple as follows:

$$T_{em} = p\left(\emptyset_{Sd}.I_{Sq} - \emptyset_{Sq}.I_{Sd}\right) \quad \text{(II.32)}$$

Or:

$$\begin{cases} T_{em} = p.\dfrac{M_{SR}}{L_R}\left(\emptyset_{Rd}.I_{Sq} - \emptyset_{Rq}.I_{Sd}\right) \\ J\dfrac{d\Omega}{dt} + \Omega f = T_{em} - T_r \end{cases} \quad \text{(II.33)}$$

II.3.2. Choice of Park's frame of reference

Following the constitution and operating principle of the DFIM, we can summarize that there are three useful choices of reference for two axes[15]:

- ✓ Stator related coordinate system: $d\theta_S/dt=0$.
- ✓ Rotor related marker: $d\theta_S/dt=\omega=p\Omega$.
- ✓ Coordinate system linked to the rotating field: $d\theta_S/dt=\omega_s$.

Where

- ✓ The first reference point is very often used in the study of observers,
- ✓ The second is widely used in the study of transient regimes of asynchronous machines,
- ✓ The latter is often used in the study and synthesis of control laws.
- ✓ The last coordinate system is integral to the rotating field, i.e. it rotates at the speed of synchronization, which translates into:

$$\frac{d\theta_s}{dt}=\omega_s \quad \text{and} \quad \frac{d\theta_s}{dt}=\omega_s-\omega_R \tag{II.34}$$

This choice allows you to define a drag pulse:

$$\omega_g=\omega_s-\omega_R \tag{II.35}$$

The formulation of the equations of the mathematical model is not simplified, and therefore keeps the form indicated by the following relations:

At the stator:

$$\begin{cases} V_{Sd}=R_S I_{Sd}+\dfrac{d\emptyset_{Sd}}{dt}-\omega_s\emptyset_{Sq} \\ V_{Sq}=R_S I_{Sq}+\dfrac{d\emptyset_{Sq}}{dt}-\omega_s\emptyset_{Sd} \\ V_0=R_S I_{S0}+\dfrac{d\emptyset_{S0}}{dt}=0 \end{cases} \tag{II.36}$$

At the rotor:

$$\begin{cases} V_{Rd}=R_R I_{Rd}+\dfrac{d\emptyset_{Rd}}{dt}-\omega_g\emptyset_{Rq} \\ V_{Rq}=R_R I_{Rq}+\dfrac{d\emptyset_{Rq}}{dt}+\omega_g\emptyset_{Rd} \\ V_0=R_R I_{R0}+\dfrac{d\emptyset_{R0}}{dt}=0 \end{cases} \tag{II.37}$$

II.4. Model of the DFIM in the form of an equation of state

For the asynchronous machine with dual feeding, the control variables are the stator and rotor voltages. Considering stator and rotor currents as state vectors, then the DFIM model is described by the following equation of state[16]:

$$\begin{cases} \dot{X} = \dfrac{dX}{dt} = AX + BU \\ Y = CX \end{cases} \tag{II.38}$$

With:

X: Status vector.

A: System state evolution matrix.

B: Order matrix.

U: Vector of the control system.

Y: Output vector,

C: Output matrix (observation matrix),

Where:

$$X = \begin{bmatrix} i_{sd} \\ i_{sq} \\ i_{rd} \\ i_{rq} \end{bmatrix}, U = \begin{bmatrix} v_{sd} \\ v_{sq} \\ v_{rd} \\ v_{rq} \end{bmatrix}, C = \begin{bmatrix} 1 & 0 & 0 & 0 \\ 0 & 1 & 0 & 0 \\ 0 & 0 & 1 & 0 \\ 0 & 0 & 0 & 1 \end{bmatrix} \tag{II.39}$$

Through a matrix representation

$$\begin{bmatrix} L_s & 0 & M & 0 \\ 0 & L_s & 0 & M \\ M & 0 & L_r & 0 \\ 0 & M & 0 & L_r \end{bmatrix} \cdot \frac{d}{dt} \begin{bmatrix} i_{sd} \\ i_{sq} \\ i_{rd} \\ i_{rq} \end{bmatrix} = \begin{bmatrix} -R_s & \omega_s L_s & 0 & \omega_s M \\ -\omega_s L_s & -R_s & \omega_s M & 0 \\ 0 & (\omega_s - \omega)M & -R_s & (\omega_s - \omega)L_r \\ (\omega_s - \omega)M & 0 & -(\omega_s - \omega)L_r & -R_s \end{bmatrix} \cdot \begin{bmatrix} i_{sd} \\ i_{sq} \\ i_{rd} \\ i_{rq} \end{bmatrix} + \begin{bmatrix} 1 & 0 & 0 & 0 \\ 0 & 1 & 0 & 0 \\ 0 & 0 & 1 & 0 \\ 0 & 0 & 0 & 1 \end{bmatrix} \cdot \begin{bmatrix} v_{sd} \\ v_{sq} \\ v_{rd} \\ v_{rq} \end{bmatrix} \tag{II.40}$$

And

$$\frac{d}{dt} \begin{bmatrix} i_{sd} \\ i_{sq} \\ i_{rd} \\ i_{rq} \end{bmatrix} = \begin{bmatrix} L_s & 0 & M & 0 \\ 0 & L_s & 0 & M \\ M & 0 & L_r & 0 \\ 0 & M & 0 & L_r \end{bmatrix}^{-1} \cdot \begin{bmatrix} -R_s & \omega_s L_s & 0 & \omega_s M \\ -\omega_s L_s & -R_s & \omega_s M & 0 \\ 0 & (\omega_s - \omega)M & -R_s & (\omega_s - \omega)L_r \\ (\omega_s - \omega)M & 0 & -(\omega_s - \omega)L_r & -R_s \end{bmatrix} \cdot \begin{bmatrix} i_{sd} \\ i_{sq} \\ i_{rd} \\ i_{rq} \end{bmatrix} + \begin{bmatrix} L_s & 0 & M & 0 \\ 0 & L_s & 0 & M \\ M & 0 & L_r & 0 \\ 0 & M & 0 & L_r \end{bmatrix}^{-1} \cdot \begin{bmatrix} v_{sd} \\ v_{sq} \\ v_{rd} \\ v_{rq} \end{bmatrix} \tag{II.41}$$

We ask:

$$[L]=\begin{bmatrix} L_s & 0 & M & 0 \\ 0 & L_s & 0 & M \\ M & 0 & L_r & 0 \\ 0 & M & 0 & L_r \end{bmatrix} \text{ et } [Z]=\begin{bmatrix} -R_s & \omega_s L_s & 0 & \omega_s M \\ -\omega_s L_s & -R_s & \omega_s M & 0 \\ 0 & (\omega_s-\omega)M & -R_s & (\omega_s-\omega)L_r \\ (\omega_s-\omega)M & 0 & -(\omega_s-\omega)L_r & -R_s \end{bmatrix} \quad \text{(II.42)}$$

$$\frac{dX}{dt}=[L]^{-1}.[Z].X+[L]^{-1}.U \quad \text{(II.43)}$$

By analogy of equation (II.10) with equation (II.7) we find:

$$A=[L]^{-1}.[Z] \quad \text{et } B=[L]^{-1} \quad \text{(II.44)}$$

In order to simplify Simulink/MATLAB's realization, the matrix [Z] can be broken down into the following form:

$$[Z]=-[Z_1]-\omega.[Z_2]+\omega_s.[Z_3] \quad \text{(II.45)}$$

With:

$$[Z]=\begin{bmatrix} R_s & 0 & 0 & 0 \\ 0 & R_s & 0 & 0 \\ 0 & 0 & R_r & 0 \\ 0 & 0 & 0 & R_r \end{bmatrix}, [Z]=\begin{bmatrix} 0 & 0 & 0 & 0 \\ 0 & 0 & 0 & 0 \\ 0 & M & 0 & L_r \\ -M & 0 & -L_r & 0 \end{bmatrix}, [Z]=\begin{bmatrix} 0 & L_s & 0 & M \\ -L_s & 0 & -M & 0 \\ 0 & M & 0 & L_r \\ -M & 0 & -L_r & 0 \end{bmatrix} \quad \text{(II.46)}$$

II.5. Modelling of the power system

II.5.1. The structure of the supply chain chosen

As shown in Figure (II.4), the machine is powered by two voltage inverters, connected to two independent DC buses, which can provide the maximum power required on each side. The switches were chosen according to the maximum current flowing through them, the voltage across them and the frequency of the inverter's carrier. PWM pulse width modulation, of the symmetrical regular sine wave type (fixed frequency sine-triangle), is adopted for the control of inverters. [14]

The DC bus is made up of a filter cell consisting of a capacitance that reduces voltage ripples at the inverter's input, an inductor to better smooth the current, and a resistor to increase the damping of the filter achieved.

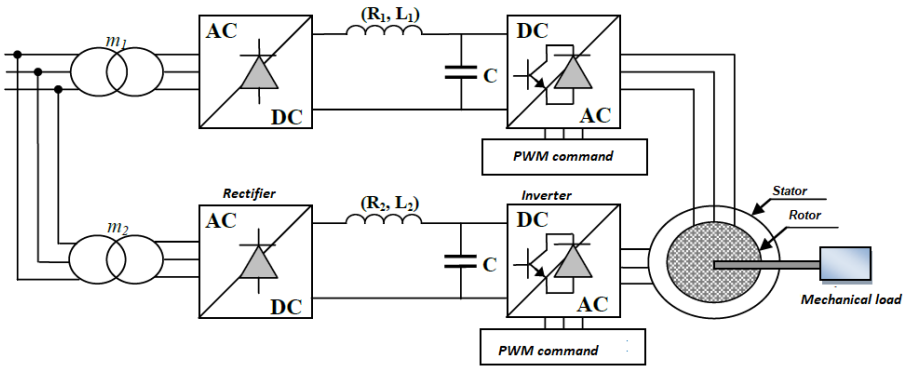

Figure II.4: Proposed synoptic diagram for feeding the DFIM[14]

II.5.2. Modeling of a three-phase double-alternating diode rectifier

Rectifiers are the converters of the power electronics that provide AC-DC conversion. Powered by an alternating voltage source, they supply direct current to the receiver connected to their output.

The rectifier used in both of the DFIM's power supplies is a three-phase double-alternating diode rectifier. Figure (II.5) represents its schematic diagram, it is composed of three diodes (D1, D2, D3) with a common cathode, each conducted when the potential of its anode is the most positive, and three diodes (D4, D5, D6) with a common anode, each conducted when the potential of its cathode is the most negative, thus ensuring the return of current $i_d(t)$. [16]

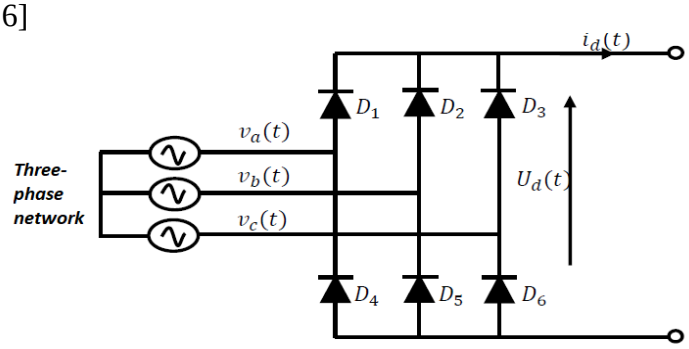

Figure II.5: Diagram of a three-phase double-alternating diode rectifier[16]

The rectifier is then powered by the following three-phase system[10]:

$$\begin{cases} v_a(t) = v_m \sin(2\pi ft) \\ v_b(t) = v_m \sin\left(2\pi ft - \dfrac{2\pi}{3}\right) \\ v_c(t) = v_m \sin\left(2\pi ft - \dfrac{4\pi}{3}\right) \end{cases} \quad \text{(II.47)}$$

The rectified voltage can be determined by:

$$u_d(t) = \max[v_a(t), v_b(t), v_c(t)] - \min[v_a(t), v_b(t), v_c(t)] \quad \text{(II.48)}$$

Its average value is given by:

$$u_d = \frac{3\sqrt{3}}{\pi} v_m \quad \text{(II.49)}$$

The voltage obtained by this rectifier has significant ripples, which requires a filter.

II.5.3. Modelling of the filter circuit:

The role of this circuit is to reduce the rate of ripples of the rectified voltage. Figure (II.6) shows its schematic diagram. [5]

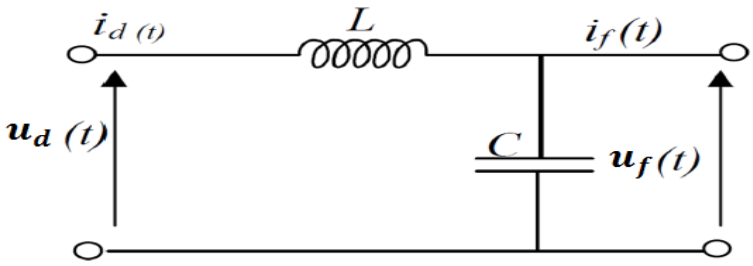

Figure II. 6: Rectified Voltage Filter Circuit[5]

This circuit can be modeled by the following system of equations:

$$\frac{di_d(t)}{dt} = \frac{1}{L}\left(u_d(t) - u_f(t)\right) \quad \text{(II.50)}$$

$$\frac{du_f(t)}{dt} = \frac{1}{C}\left(i_d(t) - i_f(t)\right) \quad \text{(II.51)}$$

Where:

u_d (t): is the rectified voltage;

u_f (t)Is the filtered voltage applied to the inverter;

The discretized form of the filter equations is convenient for a numerical simulation; it is given by:

$$i_d(t + \Delta t) = \frac{\Delta t}{L}\left(u_d(t) - u_f(t)\right) + i_d(t) \quad \text{(II.52)}$$

$$u_f(t + \Delta t) = \frac{\Delta t}{C}\left(i_d(t) - i_f(t)\right) + u_f(t) \quad \text{(II.53)}$$

Here is the expression of the transfer function of this filter:

$$F_t(s) = \frac{u_f(s)}{u_d(s)} = \frac{1}{1 + \left(\sqrt{LC}s\right)^2} \quad \text{(II.54)}$$

Where: s is the operator of LAPLACE.

This function is of the second order, its cut-off frequency being:

$$f_c = \frac{1}{\sqrt{LC}} \quad \text{(II.55)}$$

To size the filter, simply choose the cut-off frequency that is lower enough than the frequency of the first harmonic of $u_d(t)$

II.5.4. Modeling of the Voltage Inverter

A voltage inverter is a static converter that ensures the transformation of voltage from a direct source into an alternating voltage.

It consists of switching cells generally with transistors or GTO thyristors for high power.

The inverter assembly consists of six bidirectional switches, each switch consists of a transistor (T) and a diode (D) mounted head-to-toe (Figure (II.7)). The pairs of switches (K11, K21), (K12, K22), (K13, K23) are controlled in a complementary way, to ensure the continuity of the currents in the stator phases of the machine, and to avoid short-circuiting the source. Dij diodes (ij=1, 2, 3) are freewheel diodes that protect thyristors. [17]

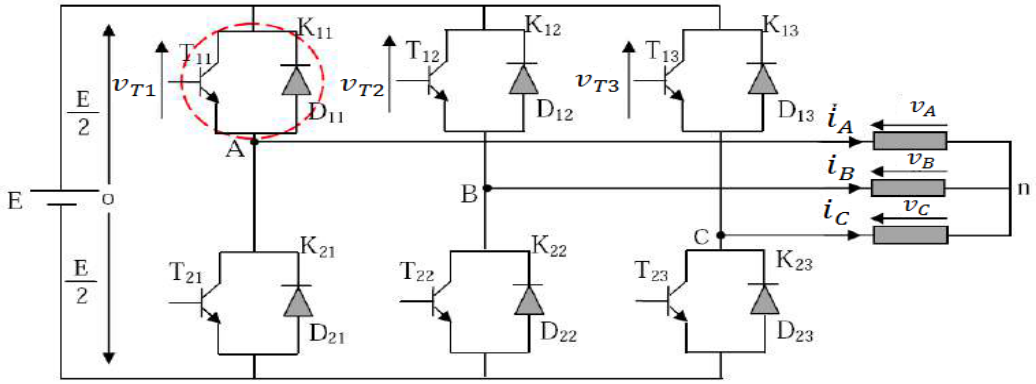

Figure II.7: Two-Level Three-Phase Voltage Inverter[17]

In controllable mode, the tonearm is a two-Formalism switch that allows you to obtain two voltage levels at the output. An arm of the inverter is shown in Figure (II.8)[18].

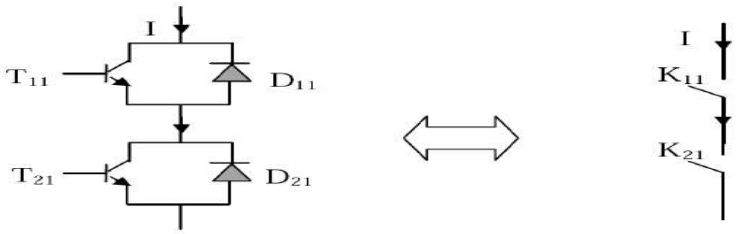

Figure II. 8: Representation of a GTO[18]

In order to avoid shorting the DC voltage source, the controls of the switches on the same arm must be complementary. To simplify the study, we will assume that the coupling is

of the star type without neutral (although the connection of a triangle load is possible). Thus the harmonics of rank three and multiples of three are eliminated, and the three-phase system obtained at the output of the inverter is a voltage-balanced three-phase system containing only the harmonics by changing three.

To obtain an alternating voltage from a DC voltage, the input voltage must be cut and applied to the load sometimes in one direction or in the other direction.

The inverter powered by a perfect voltage source imposes at its output, thanks to the opening and closing of the switches, an alternating voltage formed by a succession of rectangular slots, the operating period being fixed by the control of the switches[3].

The simple voltage equations applied to the three phases are:

$$\begin{cases} v_A = v_{AO} + v_{On} \\ v_B = v_{BO} + v_{On} \\ v_C = v_{CO} + v_{On} \end{cases} \quad \text{(II.56)}$$

By addition we have: $v_A + v_B + v_C = v_{AO} + v_{BO} + v_{CO} + 3v_{On}$

Knowing that the system of satirical three-phase voltages is symmetrical.

Therefore:

$$v_{AO} + v_{BO} + v_{CO} + 3v_{On} = 0 \quad \text{(II.57)}$$

Where from:

$$v_{On} = -\frac{1}{3}(v_{AO} + v_{BO} + v_{CO}) \quad \text{(II.58)}$$

We replace (II.53) in (II.52), we will have the following system:

$$\begin{cases} v_A = \frac{2}{3}v_{AO} - \frac{1}{3}v_{BO} - \frac{1}{3}v_{CO} \\ v_B = -\frac{1}{3}v_{AO} + \frac{2}{3}v_{BO} - \frac{1}{3}v_{CO} \\ v_C = -\frac{1}{3}v_{AO} - \frac{1}{3}v_{BO} + \frac{2}{3}v_{CO} \end{cases} \quad \text{(II.59)}$$

The system (II.15) can be written in the following matrix form:

$$\begin{bmatrix} v_A \\ v_B \\ v_C \end{bmatrix} = \frac{1}{3}\begin{bmatrix} 2 & -1 & -1 \\ -1 & 2 & -1 \\ -1 & -1 & 2 \end{bmatrix}\begin{bmatrix} v_{AO} \\ v_{BO} \\ v_{CO} \end{bmatrix} \quad \text{(II.60)}$$

With;

$$\begin{cases} v_{AO} = \frac{E}{2} F_1 \\ v_{BO} = \frac{E}{2} F_2 \\ v_{CO} = \frac{E}{2} F_3 \end{cases} \quad \text{(II.61)}$$

Such as:

$$\begin{cases} F_1 = 1 \text{ si } K_{11} \text{ fermé} \quad \text{si non} \quad F_1 = -1 \text{ donc } K_{11} \text{ ouvert}. \\ F_2 = 1 \text{ si } K_{12} \text{ fermé} \quad \text{si non} \quad F_2 = -1 \text{ donc } K_{12} \text{ ouvert}. \\ F_3 = 1 \text{ si } K_{13} \text{ fermé} \quad \text{si non} \quad F_3 = -1 \text{ donc } K_{13} \text{ ouvert}. \end{cases}$$

We replace (II.56) in (II.55), we will have the following system:

$$\begin{bmatrix} v_A \\ v_B \\ v_C \end{bmatrix} = \frac{E}{6} \begin{bmatrix} 2 & -1 & -1 \\ -1 & 2 & -1 \\ -1 & -1 & 2 \end{bmatrix} \begin{bmatrix} F_1 \\ F_2 \\ F_3 \end{bmatrix} \quad \text{(II.62)}$$

The system (II.58) represents the mathematical model of the three-phase PWM inverter. The table below shows the expressions that take simple voltages and compound voltages, depending on the open or closed state of the switches K1, K2, K3 (the states of K4, K5, K6 are respectively complementary to those de K1, K2, K3).

Table II.1: Establishing the Expressions of Simple and Compound Tensions

K_{11}	K_{12}	K_{13}	v_{AO}	v_{BO}	v_{CO}	v_A	v_B	v_C	v_{AB}	v_{BC}	v_{CA}
F	F	F	E/2	E/2	E/2	0	0	0	0	0	0
F	0	F	E/2	-E/2	E/2	E/3	-2E/3	E/3	E	-E	0
F	F	0	E/2	E/2	-E/2	E/3	-E/3	-2E/3	0	E	-E
F	0	0	E/2	-E/2	-E/2	2E/3	-E/3	-E/3	E	0	-E
0	F	F	-E/2	E/2	E/2	-2E/3	E/3	E/3	-E	0	E
0	0	F	-E/2	-E/2	E/2	-E/3	-E/3	2E/3	0	-E	E
0	F	0	-E/2	E/2	-E/2	E/3	2E/3	-E/3	-E	E	0
0	0	0	-E/2	-E/2	-E/2	0	0	0	0	0	0

II.6. Simulation of the DFIM:

To perform the simulation of the DFIM, we can transfer the model represented by the equations in the form of a block diagram structure as shown in Figure (II. 9).

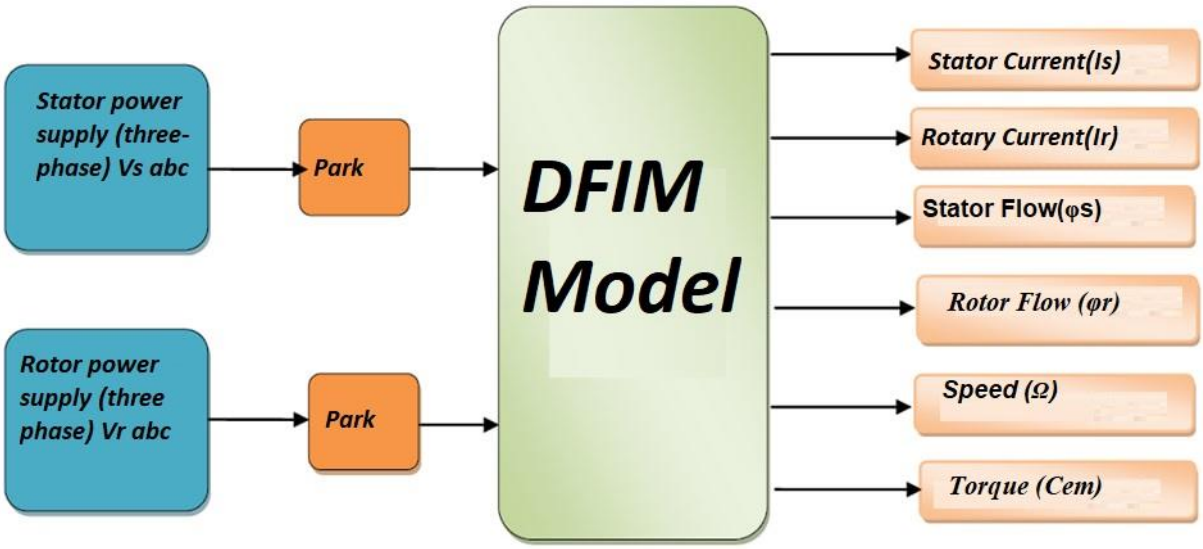

Figure II.9: DFIM Simulation Structure

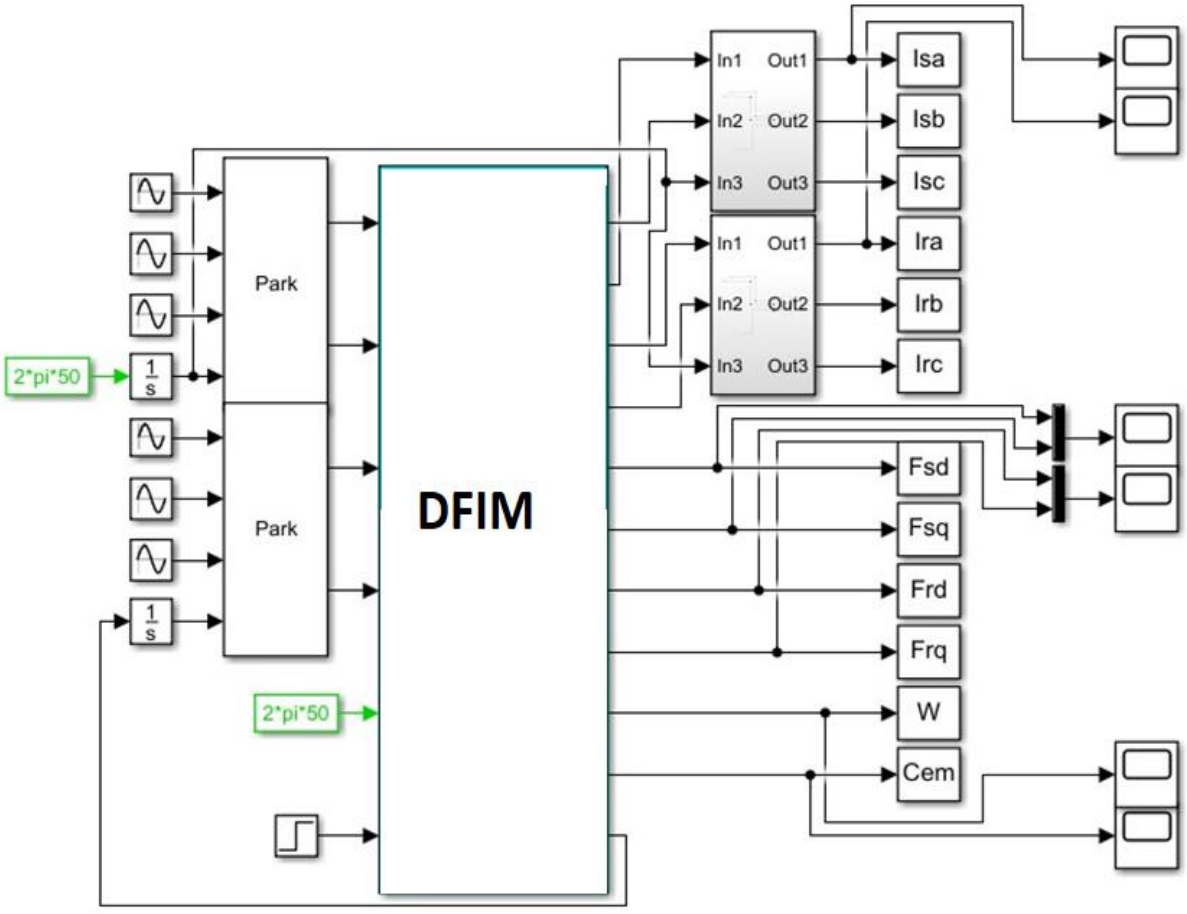

Figure II.10: DFIM simulation block diagram

II.6.1. DFIM Simulation Results:

To make the DFIM work properly, it is preferable to follow the following procedure: For the first operation, we simulated the dynamic behavior of the DFIM without a rotor power supply (short-circuited rotor), the stator being powered by a balanced three-phase network, which means that the DFIM works as an asynchronous machine with a short-circuit wound rotor.

- vr=0v, f_(r)=0Hz, (rotor short-circuited), Cr=5N.mà t =2 sec:

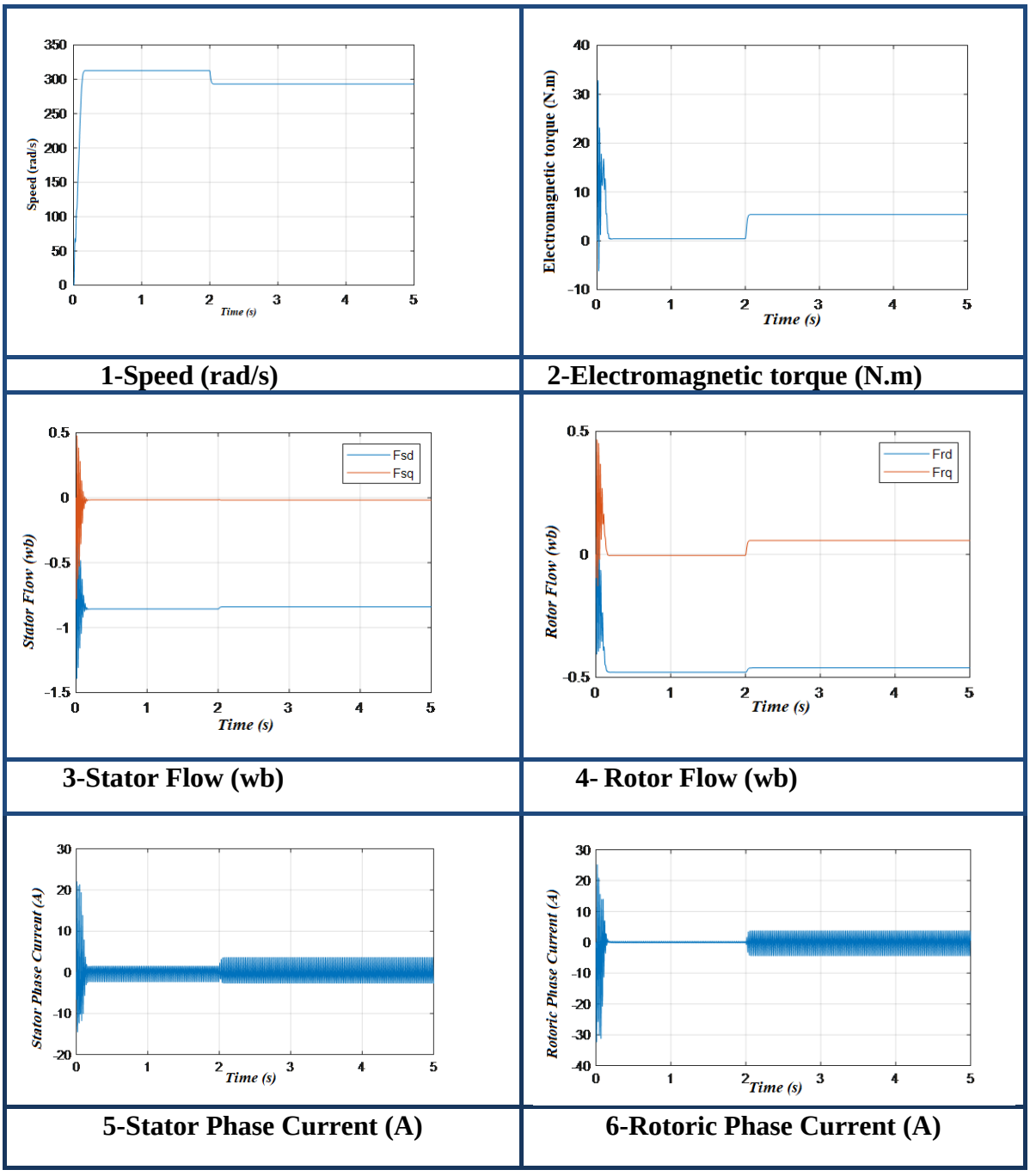

Figure II.11: DFIM Simulation Results

II.6.2. Simulation of the DFIM association with PWM inverter.

Two inverters on the rotor side and inverter on the stator side

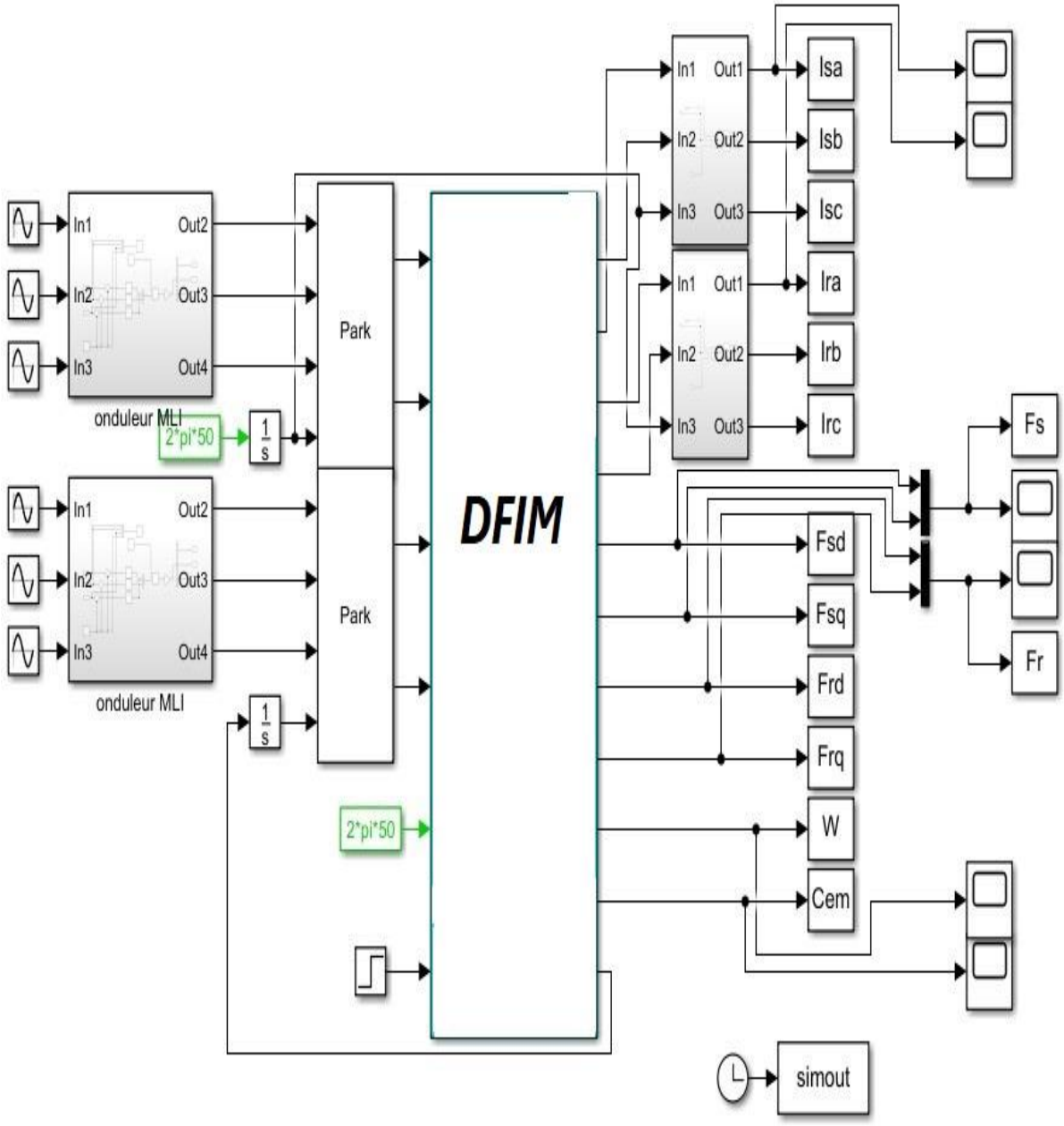

Figure II.12: Diagram of the DFIM simulation block with PWM inverter.

II.6.3. Simulation results:

Represents the simulation responses of the DFIM with a power supply by two inverters, static (220V, 50Hz) and rotoric side (Vr= 15v, fr=3Hz, at t=1s), with an application of a load torque of 5N.m at t= 2sec.

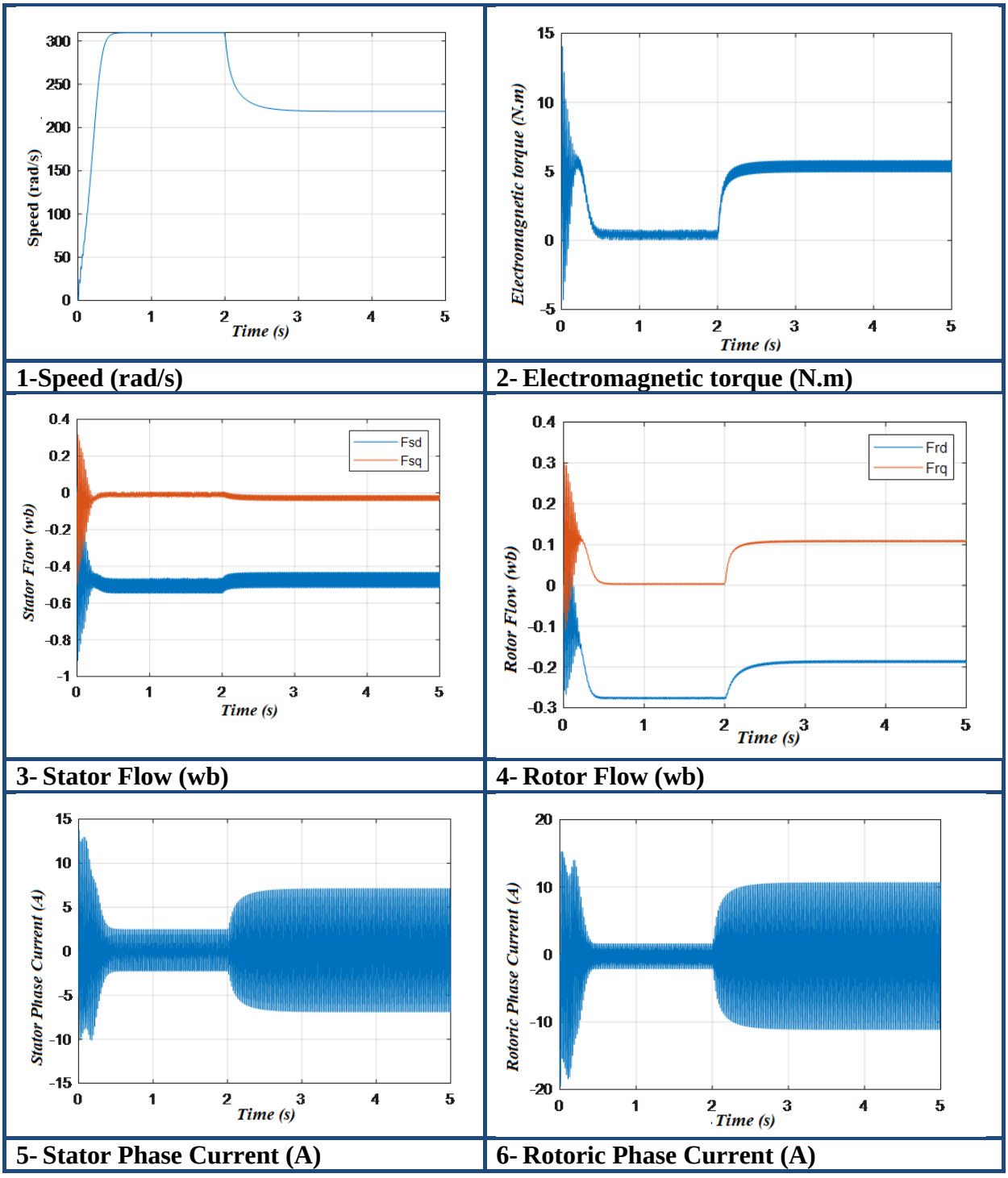

Figure II.13: Results of MADA Simulation with PWM Inverter

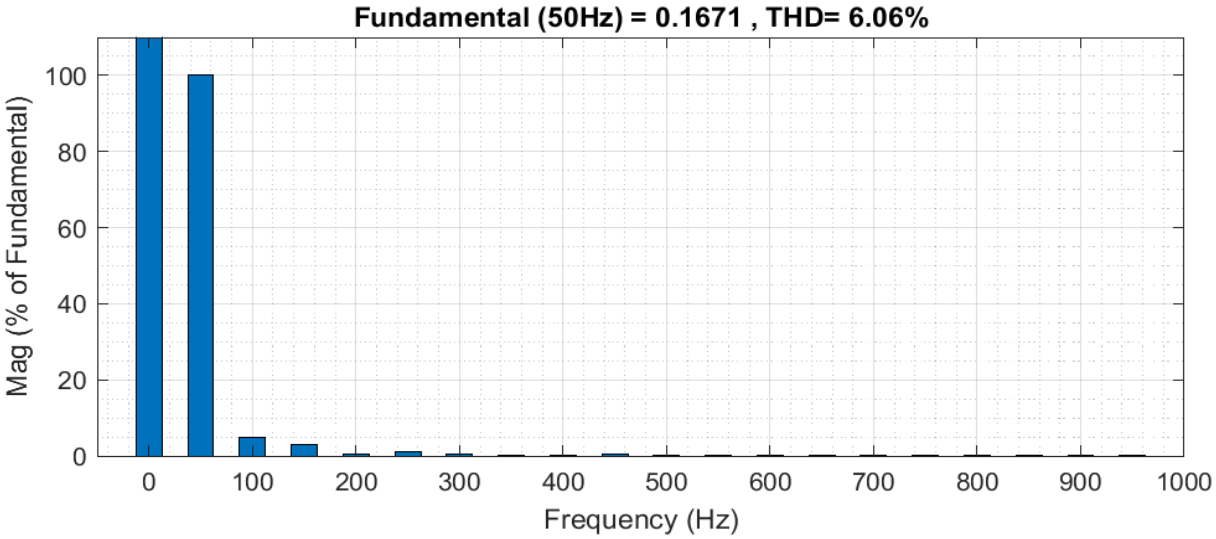

Figure II.14: Impurities at speed

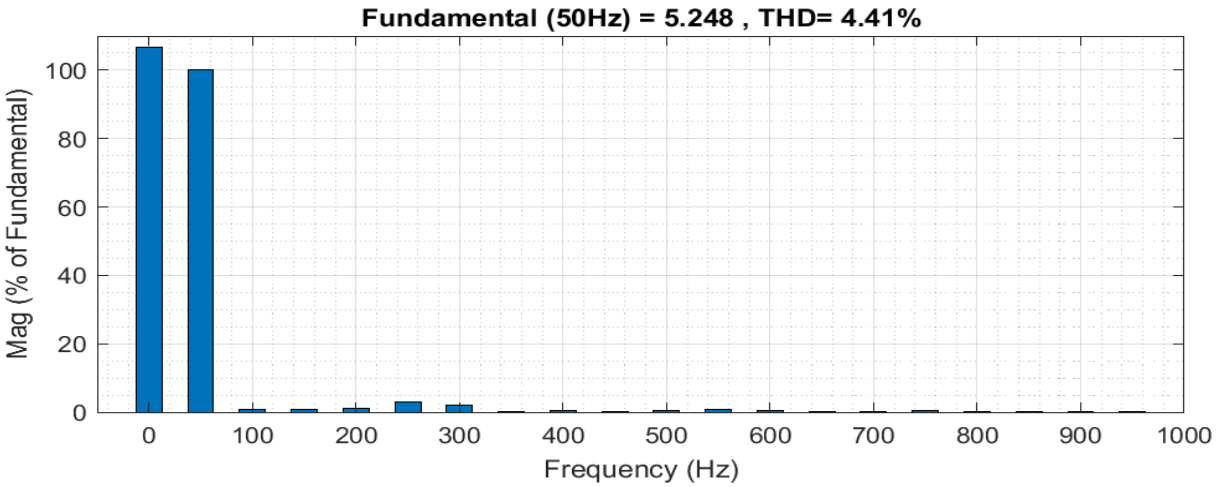

Figure II.15: Impurities at torque

When you add an inverter, we get the same results as the previous one in speed and torque, but we notice an increase in impurities when torque and Speed.

II.7. Conclusion

In this chapter, a brief study has been presented on the asynchronous machine with doubly feeding, its structure, its operating principle and the different strategies of its control; as well as its advantages, disadvantages and areas of application. We also presented the real model of the machine to which we applied the Park transformation to make it linear and more adapted to the order. Then, we modeled the power system which includes the rectifier, the filter and the inverter. For the latter, the PWM technique was applied to control it and Simulation of the asynchronous machine with doubly power supply and Simulation of the DFIM association with PWM inverter.

Chapter III

Direct Torque Control (DTC) of the doubly fed induction machine

III.1. Introduction

In mid 1980s, innovative studies have been carried by Depenbrock [6],[7] and by both Isao Takahashi and Toshihiko Noguchi[10].Those studies proposed a new concept of control for A.C machine which is the direct torque control.

DTC of an induction motor has been successful because it explicitly considers the inverter stage and uses few machine parameters, while being more robust to parameter uncertainty than field-oriented control [4].

Therefore, there are lots of questions which need to be investigated further in this aspect.

In this chapter, we were interested in the order of the DTC applicable to the rotor adapter and Principle of DTC control and Operation of a three-phase voltage inverter and control of stator flow and electromagnetic torque and Choice of voltage vector and estimators and Elaboration of the control vector and elaboration of the control table.

III.2. General Structure of The DTC

The general principle of DTC work shown in the Figure (III.1)

- stator flux and torque are calculated
- reference torque is calculated from reference speed and actual speed of the motor
- the reference stator flux magnitude and the torque are compared with the estimated flux magnitude and torque and the flux error and torque error are delivered to the hysteresis controller

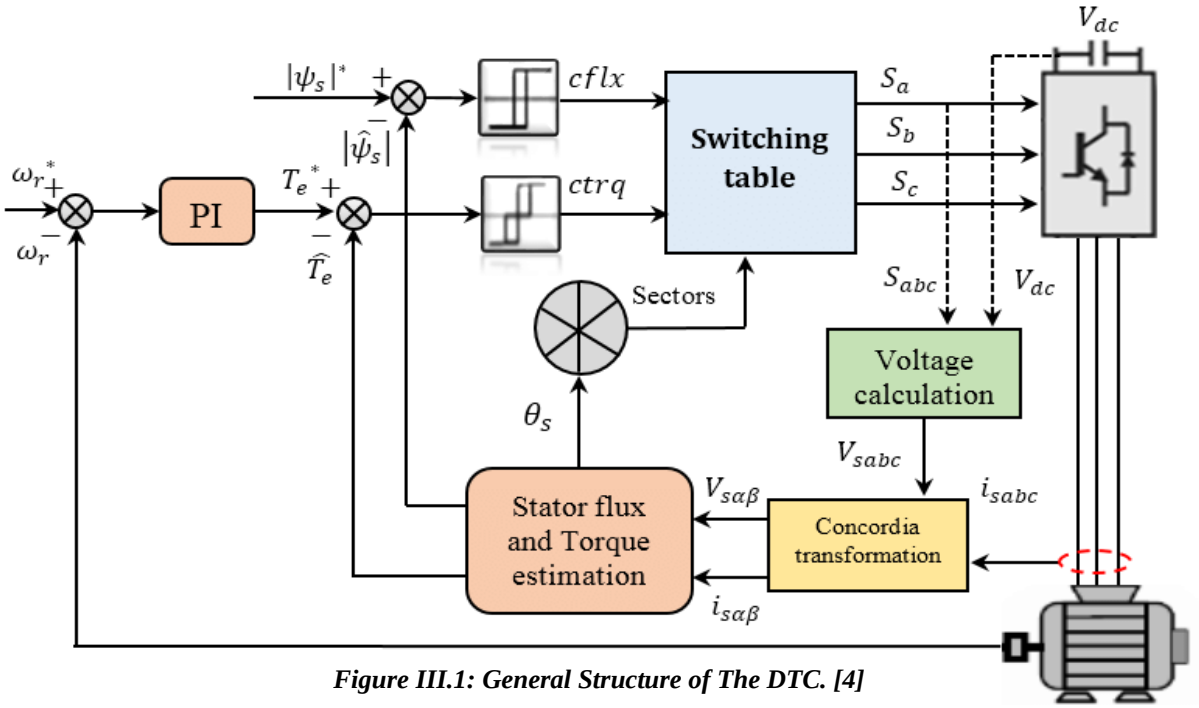

Figure III.1: General Structure of The DTC. [4]

Direct torque control (DTC) uses the voltage vector instantaneous values and is dependent on the stator flux direction. Two of the eight instantaneous base voltage vectors that a three-phase inverter can produce are zero. Based on the position of the stator flux vector, flux and torque errors, and other factors, these vectors are chosen from a commutation table. Thus, DTC stands out as a technique that can run alternating current devices without requiring the use of mechanical sensors. [19]

The model yields the following values at each moment based on measurements of the DC

voltage at the inverter's input and the currents of the stator phases:

- The motor's real stator flux
- The actual torque it generates
- The position of the sector

III.3. Principle of the DTC order

The DTC direct torque control methods consist of directly controlling the closing or opening of the inverter switches from the calculated values of the stator flux and torque. [19]

The control variables are the magnetizing flux and the torque of the motor. With DTC, we don't need a modulator, or a tachometer or a position encoder to ensure speed or position feedback.

The control of the switches is intended to give the vector representing the stator flow the direction determined by the set values.

To know the electromagnetic state of the motor in order to determine the control of the inverter switches, a similar model of the machine is required.

Based on the measurements of the DC voltage at the inverter input and the stator currents, the main characteristic models of a direct torque control The complete characteristics of a direct torque control are:

- The direct torque control is based on the selection of the optimal inverter switching vectors.
- Indirect control of the machine's currents and voltages.
- gain flows and currents close to sinusoidal shapes.
- The dynamic torque response of the machine is very fast.
- The existence of the oscillations of the torque which depends on the width of the bands of the hysteresis comparators given at each instant

Measuring shaft speed is not a duty, which is a great advantage of these methods.

The flow and torque calculated in this way are compared to their reference values to determine the control times of the switches. Ordinarily, the aim is to maintain the stable flow [20]

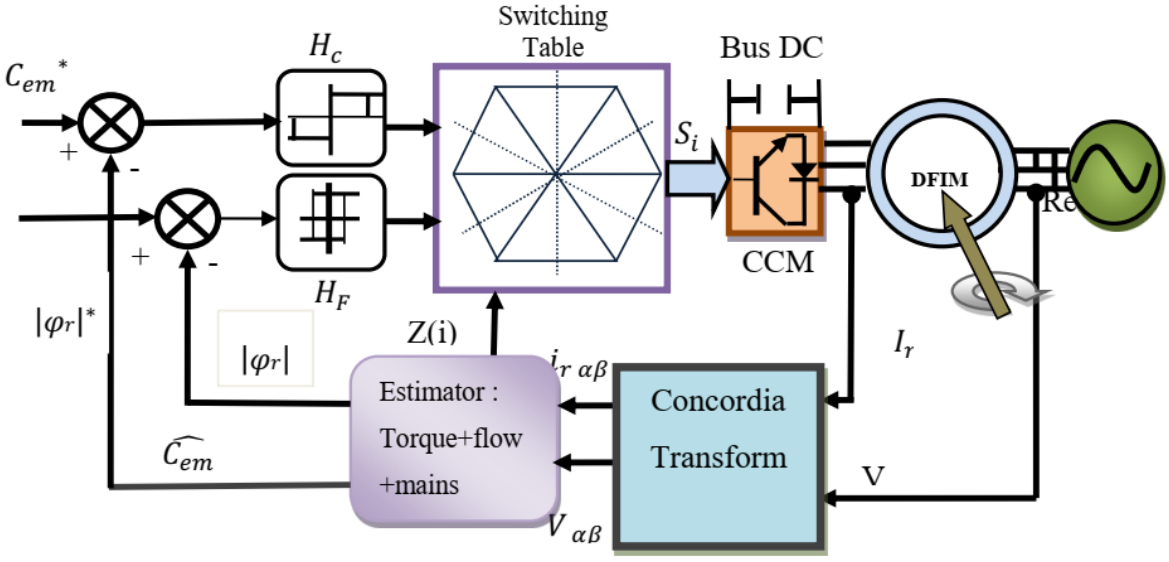

Figure III.2: Principle of the DTC order[20]

III.4. Operation of a three-phase voltage inverter

The switches of the voltage inverter must be controlled in such a way as to maintain the flow and torque of the machine. The vector of the stator tension *Vs* can be written as[15]:

$$Vs=\sqrt{\frac{2}{3}}U_0[S_a + S_b e^{j\frac{2\pi}{3}} + S_c e^{\frac{4\pi}{3}}] \quad \text{(III.1)}$$

Where $(S_a.S_b.S_c)$ represent the logical state of the 3 switches: Si=1 means that the up switch is closed and the bottom switch is open, $\left(V_i = +\frac{U_0}{2}\right)$ and Si=0 means that the top switch is open and the bottom switch is closed $\left(V_i = -\frac{U_0}{2}\right)$

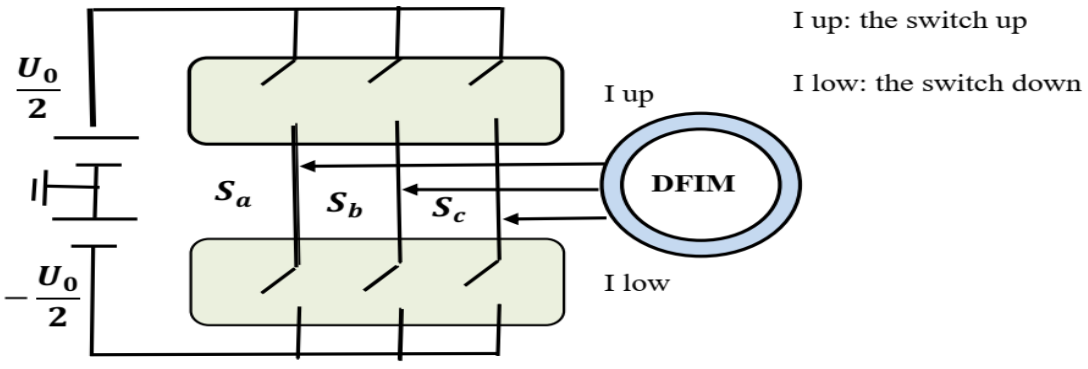

Figure III.3: Asynchronous machine controlled by voltage inverter[15]

We will therefore seek to control the flux and the torque via the choice of the voltage vector which will be done by a configuration of the switches as we have three switches there are therefore 2^3=8 possibilities for the vector V_s.

Two vectors V_0 and V_7 correspond to the null vector: (S_a, S_b, S_c) = (0, 0.0) et (S_a, S_b, S_c)=(1,1,1).

V_0 (0,0,0) is always next to an odd vector, V_1 (1,0,0); V_3 (0,1,0); where V_5 (0,0,1); hence a single switch.

V_7 (1,1,1) is always next to an Even vector; V_2 (1,1,0); V_4 (0,1,1); where V_6 (1,0,1); so a single switch.

In each modulation period, an arm does not switch twice.

Shows the representation in the complex plane of the six non-zero voltage vectors that can be generated by a two-stage three-phase voltage inverter:

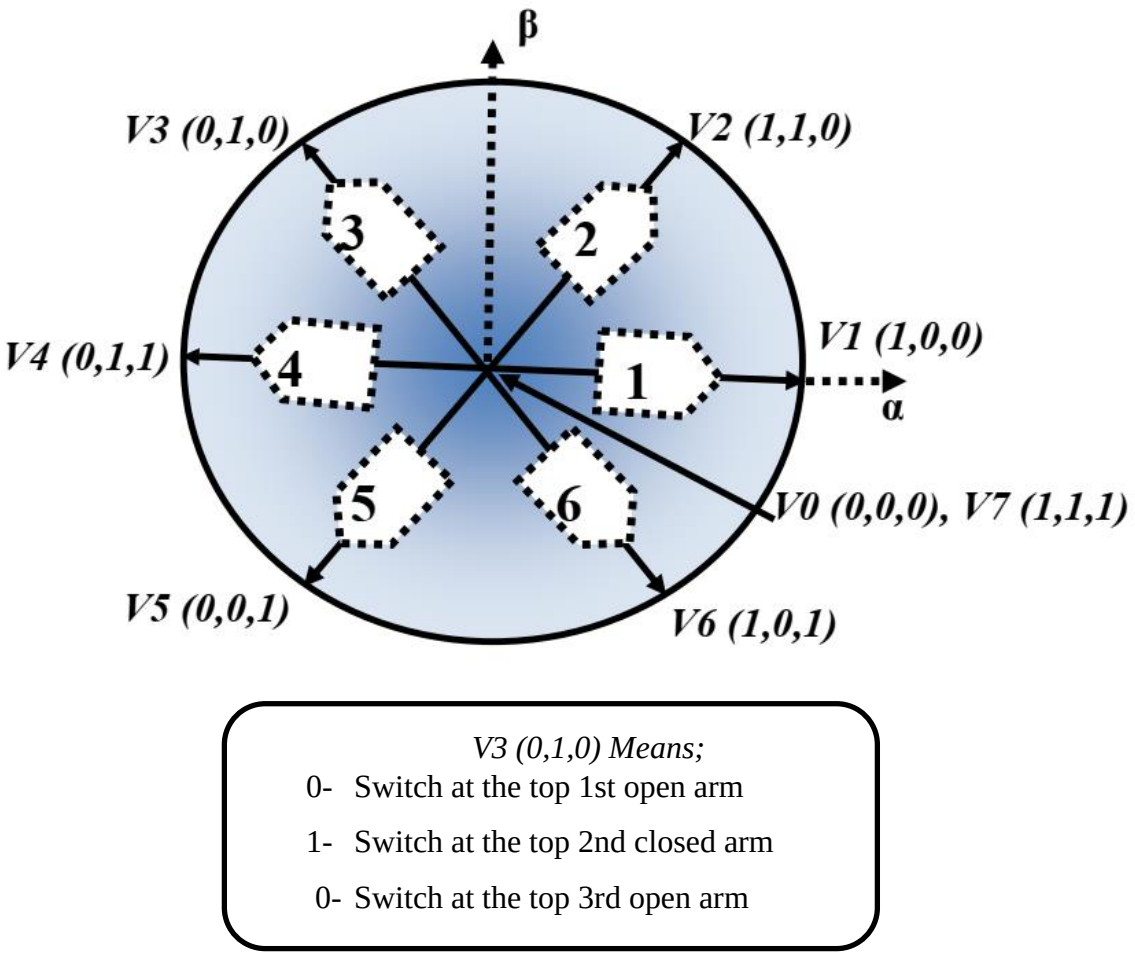

Figure III. 4: Operating Sequences of a Two-Level Voltage Inverter

III.5. Control of stator flow and electromagnetic torque

III.5.1. Principle of Stator Flow Control

From the model of the asynchronous machine in a frame linked to the stator and the expression of the stator voltage:

$$V_{s=}R_sI_s + \frac{d\varphi_s}{dt} \quad \text{(III.2)}$$

The stator flux is estimated from the following relationship:

$$\varphi_s(t) = \int_0^t (V_s - R_sI_s)dt \quad \text{(III.3)}$$

$$\varphi_s(t) = \varphi_{s0} + \int_0^t V_s\,(t) - R_s \int_0^t I_s dt \quad \text{(III.4)}$$

With the assumption that R_s remains constant and that the term (R_s. I_s) Is negligible in front of the voltage V_s over a periodic control interval [0 T_e] Suitable for a sampling period Te the commands (S_a, S_b, S_c) are fixed, so we can write [20]:

$$\varphi_s(t) \approx \varphi_{s0} + V_sT_e \quad \text{(III.5)}$$

T Where Øso: is the flux vector at time t = 0.

In a time, interval T_e, the end of the vector $\emptyset_s$ moves along a straight line whose direction is given V_s. Figure (III.5) This principle appears when we select the vector $V_s = V_3$ for example

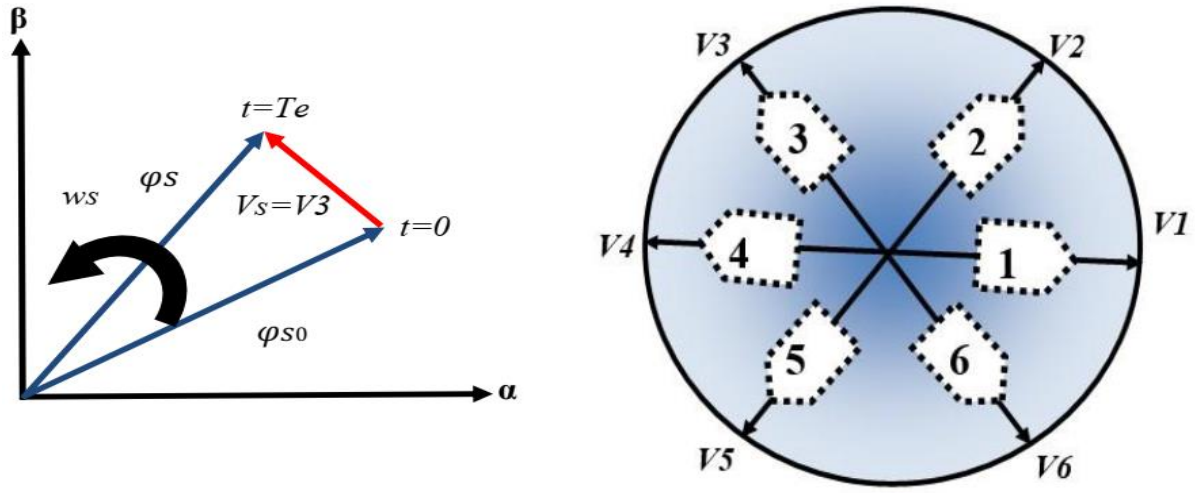

Figure III.5: Evolution of stator flux vector in the complex [21].

If the control period «T_e» is very small compared to the rotation period of the stator flux vector. By choosing a harmonious sequence of voltage vector of the inverter over successive time intervals of duration T_e, we can therefore make the end of the flow vector follow φ_sla desired trajectory [21].

The φ_s vector is maintained between two φ_{max} and φ_{min} values, with the transition from one to the other being controlled by V_s. If the control vector is one of the non-zero vectors, φ_s evolves with a constant speed proportional to the control voltage. If φ_s is kept more or less constant, the torque depends only on the phase shift between the two flows. To meet a demand for rapid torque disparity, it is therefore sufficient to quickly change the phase shift between the two flows.

For example, when φ_s reaches the φ_{max} value, the switch change is triggered so that the new V_s value causes the φ_s modulus to decrease. At the same time, the new phase of the V_s vector causes the shift Is and φ_s in the direction of rotation, increases the phase shift and torque. When φ_s drops to the φ_{min} value, the following change will be ordered.

It is possible to operate with a virtually constant φ_s flow module; To do this, simply choose a circular path for the end of the flux vector. This is not possible.

Only if the control period is very small in front of the rotation period of the flow. In addition, the component of the flow of applied voltage vectors must be minimum and on the contrary that of the torque component must be maximum. Thus the applied vectors change the position of the flow with an almost constant amplitude.

When the voltage direction V_s is nonzero, the direction of displacement of the end of the flux φ_s and given by its derivative ($d\varphi_s/dt$) practically corresponding to the vector V_s. As far as the rotor flux φ_r is concerned, it can be assumed that, given the high time constant of the rotor of the asynchronous machine, its amplitude does not vary during a transient regime. So the rate of rotor flow is negligible compared to that of the stator flow. [22]

III.5.2. Electromagnetic torque control principle

The electromagnetic torque is followed by the vector resultant between the vectors of the stator and rotor fluxes according to the following expression[20]:

$$T_{em}=k(\overline{\varphi_s} * \overline{\varphi_{\dot{r}}}) = k|\overline{\varphi_s}||\overline{\varphi_{\dot{r}}}|\sin(\Upsilon) \quad \text{(III.6)}$$

With :

$\overline{\varphi s}$: represents the stator flux vector;

$\overline{\varphi_{\dot{r}}}$: represents the rotor flux vector reduced to the stator;

Υ: represents the angle between the vectors of the stator and rotor flows.

$$k = \frac{pM}{\sigma L_s L_s} \tag{III.7}$$

According to this expression, the torque depends on the amplitude of the two vectors $\overline{\varphi s}$ and $\overline{\varphi_{\dot{r}}}$ and their relative position.

III.6. Choosing the voltage vector

The changes in the electromagnetic torque can be controlled only from the rotational speed of the flux vector $\overline{\varphi s}$, Table (III.1) shows the evolution of the two quantities flux and torque for each of the four vectors V_{i+1}, V_{i+2}, V_{i-1}, V_{i-2} which can be applied in zone *i*.

When the flux $\overline{\varphi s}$ is in a zone *i*, the control of the flux and torque can be ensured by selecting one of the following eight voltage vectors[23]:

- If V_{i+1} is selected then the amplitude of the flux φ_s increases and the torque T_{em} increases
- If V_{i-1} is selected then the flux amplitude $\overline{\varphi s}$ increases and the Tem pair decreases
- If V_{i+2} is selected then the amplitude of the flux $\overline{\varphi s}$ decreases and the pair T_{em} increases
- If V_{i-2} is selected then the flux amplitude $\overline{\varphi s}$ decreases and the T_{em} torque decreases
- If V_0 or V_7 is selected, the rotation of $\overline{\varphi s}$ is stopped, resulting in a decrease in torque

While the torque module remains unchanged.

The voltage vectors to be applied depend on the area where the flux vector is located.

Table III.1: Evolution of the flux and torque quantities as a function of the vector Vs applied in zone i

Vector Vk	$Vi+1$	$Vi+2$	$Vi-1$	$Vi-2$
φ_s	↗	↘	↗	↘
T_{em}	↗	↘	↘	↘

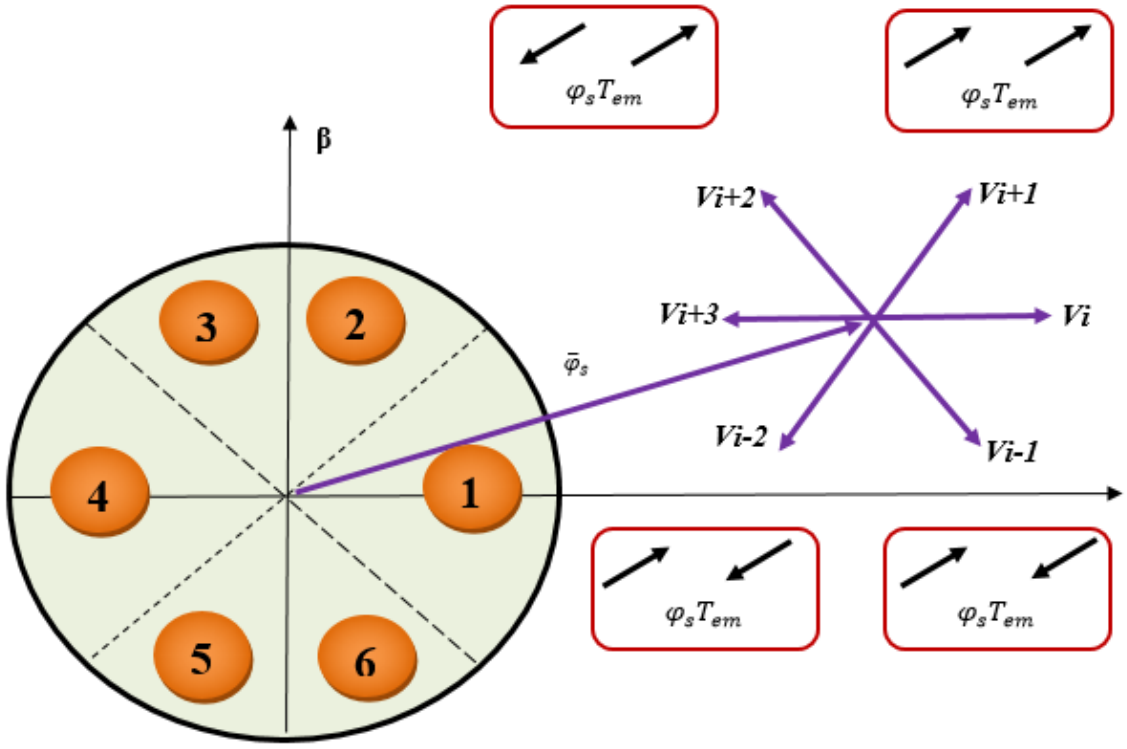

Figure III. 6: Area Distribution [21]

The level of efficiency of applied voltage vectors also depends on the position of the flux vector in zone *i*.

As a result, at the beginning of the zone, the vectors $\overline{Vi+1}$ and $\overline{Vi-2}$ are perpendicular to $\overline{\varphi s}$, hence a rapid evolution of the torque but a slow evolution of the amplitude of the flux $\varphi\bar{\bar{s}}$, while at the end of the zone the evolution is the opposite. With the vectors $\overline{Vi+1}$ and $\overline{Vi-2}$, it corresponds to slow and rapid changes in the amplitude of the flux $\overline{\varphi s}$ at the beginning of the zone, whereas at the end of the zone it is the opposite. [20]

Regardless of the direction of change in torque or flux, in zone i, the two vectors Vi and $\overline{Vi+3}$ are never used. Indeed, these have the strongest flux component (very rapid evolution of $(\varphi s)\bar{}$) but the effect on the torque depends on the position of $\overline{\varphi s}$ in the zone, with a zero effect in the middle of the zone. The voltage vector at the output of the inverter is deduced from the torque and flux deviations, estimated from their reference, as well as the position of the vector $\overline{\varphi s}$.[24]

An estimator of $\overline{\varphi s}$ in modulus and position as well as a torque estimator are therefore required.

III.7. Estimators

III.7.1. Estimation of stator flux

The flow can be calculated from measurements of the current stator quantities and the voltage of the machine. [24]

From the equation:

$$\overline{\varphi s} = \int_0^t (\overline{V_s} - R_s \overline{I_s}) dt \tag{III.10}$$

We obtain the components α and β of the vector φs

$$\begin{cases} \varphi_{s\alpha} = \int_0^t (V_{s\alpha} - R_s I_{s\alpha}) dt \\ \varphi_{s\beta} = \int_0^t \left(V_{s\beta} - R_s I_{s\beta}\right) dt \end{cases} \tag{III.11}$$

These equations represent the century of calculation necessary to estimate the amplitude of the stator flux.

The voltages $V_{s\alpha}$ and $V_{s\beta}$ are obtained from the controls (S_a, S_b, S_c) and the measurement of the voltage U_{dc} and by applying the Concordia transform:

$$\overline{V_s} = V_{s\alpha} + jV_{s\beta} \tag{III.12}$$

$$\begin{cases} \mathrm{V}_{S\alpha} = \sqrt{\frac{2}{3}} U_{dc} \left(S_a - \frac{1}{2}(S_b + S_c) \right) \\ V_{s\beta} = \sqrt{\frac{1}{2}} U_{dc} (S_b - S_c) \end{cases} \tag{III.13}$$

Similarly, the currents $I_{s\alpha}$ and $I_{s\beta}$ are obtained from the measurement of the real currents Isa, I_{sb}, I_{sc} and by applying the Concordia transform:

$$\overline{I_s} = I_{s\alpha} + jI_{s\beta} \tag{III.14}$$

$$\begin{cases} I_{s\alpha} = \sqrt{\frac{2}{3}} I_{sa} \\ I_{s\beta} = \frac{1}{\sqrt{2}}(I_{sb} - I_{sc}) \end{cases} \quad \text{(III.15)}$$

The modulus of the stator flow is written:

$$\varphi_s = \sqrt{\varphi_{s\alpha}^2 + \varphi_{s\beta}^2} \quad \text{(III.16)}$$

The angle αs between the stator frame of reference and the flux vector φs is equal to:

$$\alpha_s = arctg \frac{\varphi_{s\beta}}{\varphi_{s\alpha}} \quad \text{(III.17)}$$

III.7.2. Electromagnetic torque estimation

The electromagnetic torque can be estimated from the estimated fluxes, and the measured stator currents, and which can be put in the following form[23]:

$$T_{em} = p\left(\varphi_{s\alpha} i_{s\beta} - \varphi_{s\beta} i_{s\alpha}\right) \quad \text{(III.18)}$$

It can be noted in this equation that the accuracy of the latter depends on the quality of the flux estimation and the precision of the measurement of the stator currents.

III.8. Elaboration of the control vector

III.8.1. Flow corrector

The purpose of this correction is to maintain the amplitude of the stator flux in a band and thus to maintain the end of the latter in a circular crown as shown in (Figure III.7). [25]

The output of the verifier must indicate the direction of evolution of the module of $\overline{\varphi s}$, in order to select the corresponding voltage vector. For this, a simple two-stage hysteresis corrector is perfectly suitable, and also allows you to obtain very good dynamic performance.

The output of the corrector, represented by a Boolean variable C_{flx} directly indicates whether the amplitude of the flow should be increased (C_{flx} =1) or decreased (C_{flx} =0) in order to maintain[24]:

$$\left|\varphi_{sref} - \varphi_s\right| \leq \Delta\varphi_s \quad \text{(III.19)}$$

With:

φ_{sref} : is the reference flow.

$\Delta\varphi_s$: is the hysteresis width of the corrector.

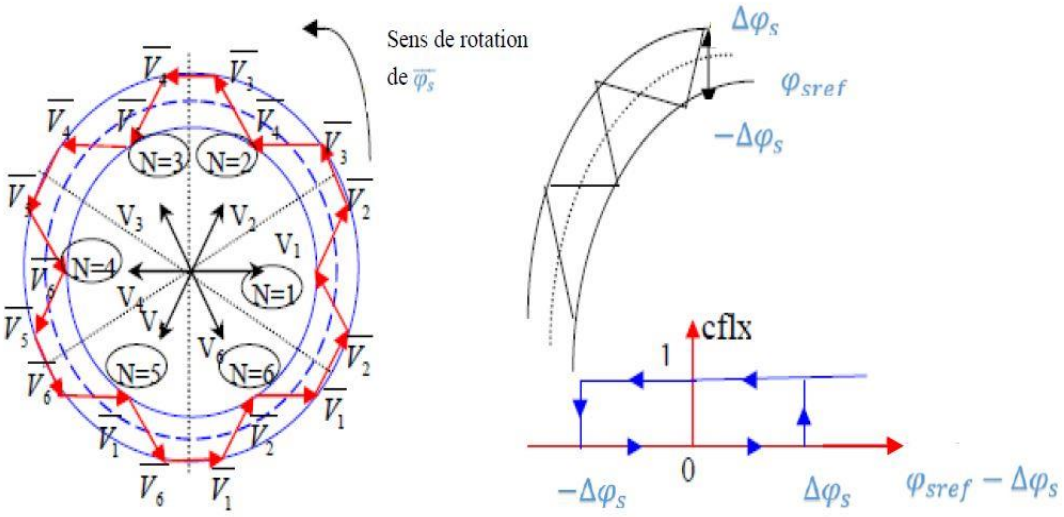

Figure III.7: Flux corrector with hysteresis and selection of the corresponding voltage vectors. [24]

III.8.2. Torque corrector

The torque examiner's goal is to keep the torque in its hysteresis band and thus to impose the amplitude of the torque's undulations within the limits[25]:

$$\left|T_{ref} - T_{em}\right| \leq \Delta T \qquad \text{(III.19)}$$

With:

T_{ref}: is the reference torque.

ΔTe: is the corrector hysteresis band.

However, a difference with flux control is that the torque can be positive or negative depending on the direction of rotation of the machine.

Two solutions can be envisaged:

- A three-level hysteresis corrector.
- A two-level hysteresis corrector.

III.8.3. Two-level corrector

The lonely vectors $\overline{V\iota + 1}$ and $\overline{V\iota + 2}$, can be selected to evolve the flux φs. Therefore, the decrease in torque is only achieved by the selection of null vectors.

However, this concealer is easier to anchor. In addition, by correctly selecting the null vectors according to the N_i zones, we can see that for each zone i, there is an arm of the

inverter that never switches, and thus allows to reduce the average switching frequency of the switches, thus reducing the switching losses at the level of the inverter. [23]

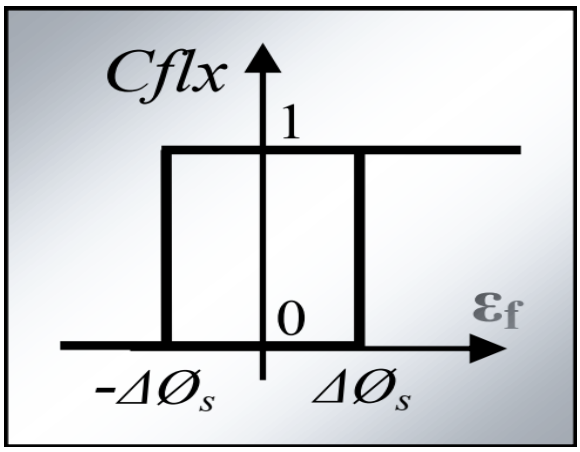

Figure III.8: Two-level Flux corrector. [23]

III.8.4. Three-level corrector

It allows the motor to be controlled in both directions of rotation, either for positive or negative torque. The output of the corrector, represented by the Boolean variable, directly indicates whether the torque amplitude should be increased in absolute value (*ccpl=1* for a positive setpoint and *ccpl= -1* for a negative setpoint) or decreased (*ccpl=0*). [25]

La figure III. 8 Shows this type of corrector.

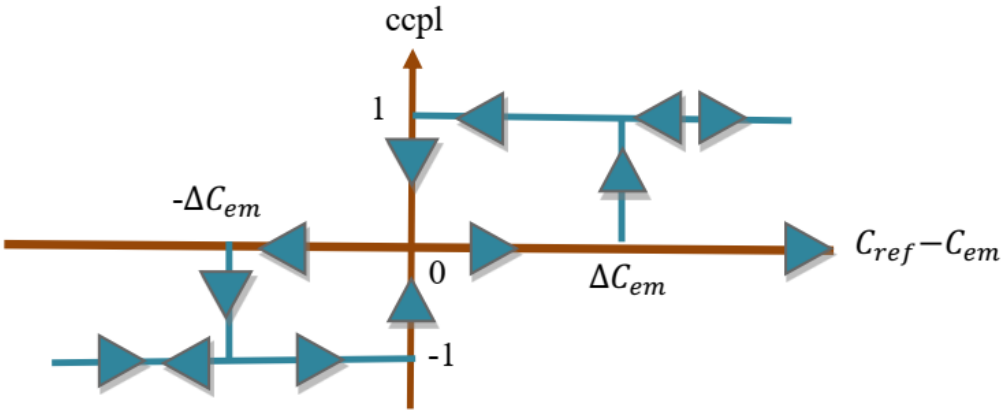

Figure III.9: Three-level Flux corrector[25]

III.8.5. Elaboration of the commutation table

The control table is constructed according to the state of the variables C_{flx} and ccpl, and the position zone *i* of φs. It is therefore presented in the following form:

Table III.2: Control strategy with a three-level hysteresis comparator (with non-zero voltage vectors).

Flow	*Couple*	N=1	N=2	N=3	N=4	N=5	N=6	*Corrector*
cflx=0	ccpl=1	V3	V4	V5	V6	V1	V2	*Two levels*
	ccpl=0	V0	V7	V0	V7	V0	V7	
	ccpl=-1	V5	V6	V1	V2	V3	V4	*Three levels*
cflx=1	ccpl=0	V2	V3	V4	V5	V6	V1	*Two levels*
	ccpl=1	V7	V0	V7	V0	V7	V0	
	ccpl=-1	V6	V1	V2	V3	V4	V5	*Three levels*

Table III.3: Control strategy with a three-level hysteresis comparator (with non-zero voltage vectors).

Flow	*Couple*	N=1	N=2	N=3	N=4	N=5	N=6	*Correcteur*
cflx=0	ccpl=1	V3	V4	V5	V6	V1	V2	*Two levels*
	ccpl=0	V4	V5	V6	V1	V2	V3	
	ccpl=-1	V5	V6	V1	V2	V3	V4	*Three levels*
cflx=1	ccpl=0	V2	V3	V4	V5	V6	V1	*Two levels*
	ccpl=1	V1	V2	V3	V4	V5	V6	
	ccpl=-1	V6	V1	V2	V3	V4	V5	*Three levels*

III.9. Conclusion

The work that appears in this chapter shows the feasibility of applying the DTC control technique on a dual feeding machine. This chapter has made it possible to study Principle of DTC control and Operation of a three-phase voltage inverter and Control of stator flow and electromagnetic torque and Choice of voltage vector and Estimators and Elaboration of the control vector and Elaboration of the control table, the behavior of the direct control of the torque of the asynchronous machine with dual power supply fed by two two-level voltage inverters.

Direct torque control has many important advantages (simplicity, ease of installation, durability, high dynamics, precision, ... etc.).

Chapter IV

Direct Torque Control simulation

IV.1. Introduction

In this chapter we will present the general architecture of the direct torque control of the Asynchronous Machine with Doubly Fed. We will go through the order developed as well as the different steps followed to validate it by simulation. General structure of the simulation.

This end describes the implementation, under the Matlab/Simulink environment, of the control strategy of the DFIM Doubly Fed Asynchronous Machine. The circuit is made up of 6 main systems:

- The electromechanical system.
- The Power System
- Switching tables.
- The system for calculating reference flows.
- The system for calculating estimated flows.
- The control system.
- The system for calculating reference angles.

IV.2. General structure of direct torque control

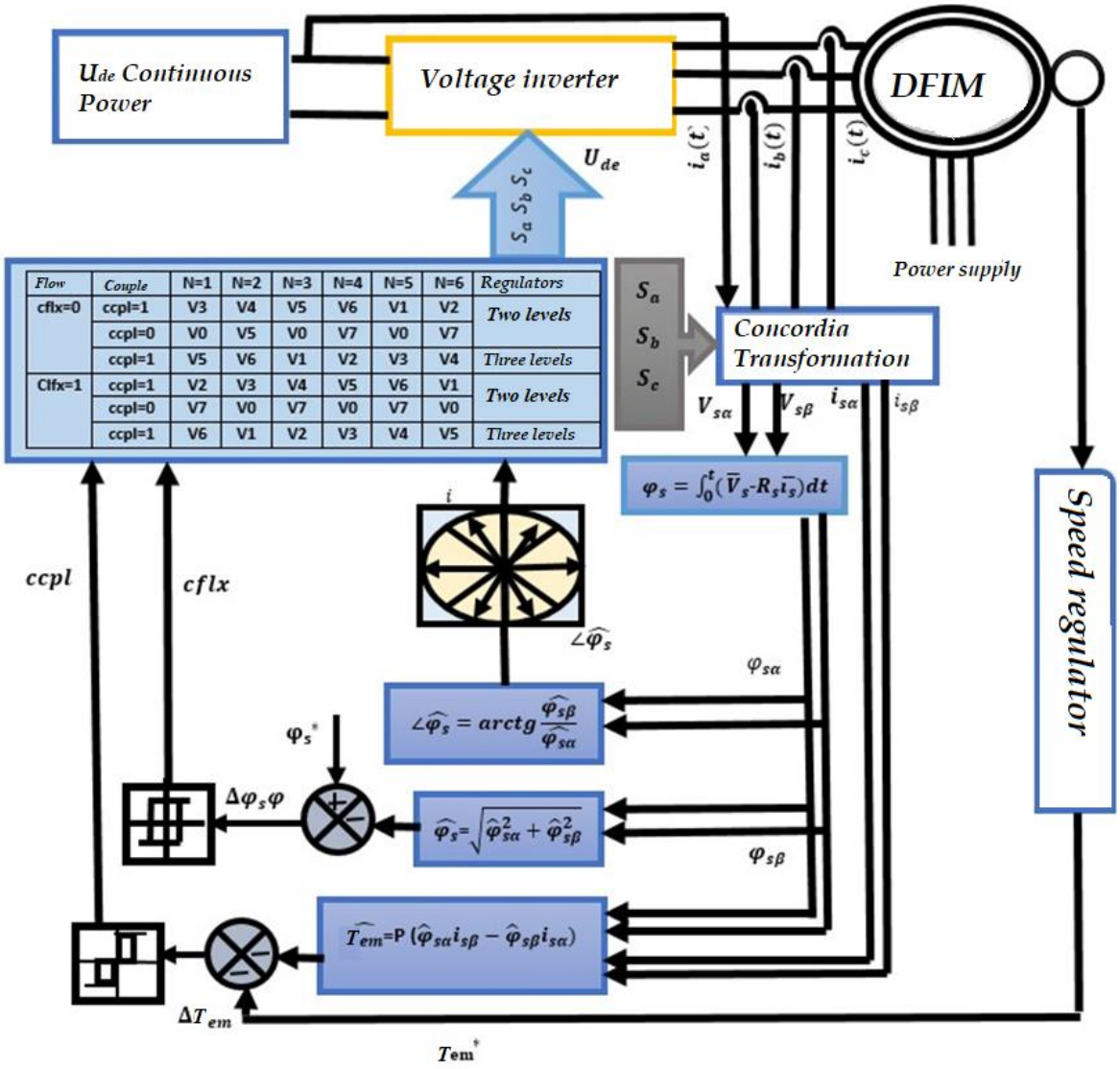

Figure IV.1: General structure of direct torque control.

IV.2.1. DFIM DTC simulation results:

In this section, we present the simulation of the doubly fed asynchronous machine with direct torque control.

In order to determine and evaluate the performance of the implemented control, a speed and torque trajectory was designed. The latter is defined as the speed set point of our machine.

IV.2.2. Variation of speed and load torque:

Time (s)	0	1.5	3	4.5
Wref (rad.sec)	125.6	115.6	105.6	65.6

Table IV.1: Variation in speed

Time (s)	0	1	2	3
Cr (N.m)	0	12.5	-25	15

Table IV.2: Load torque variation

IV.2.3. Empty start:

Results Empty Start

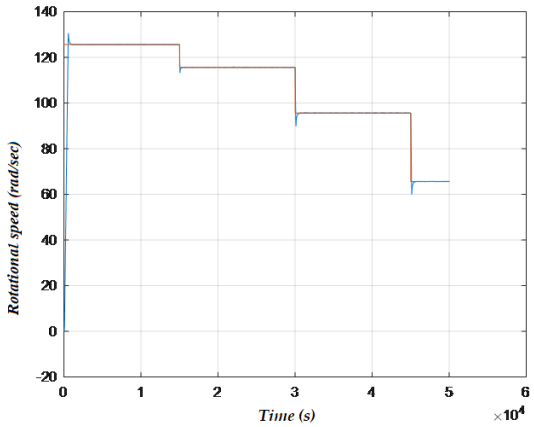

Figure IV. 2: Rotational speed

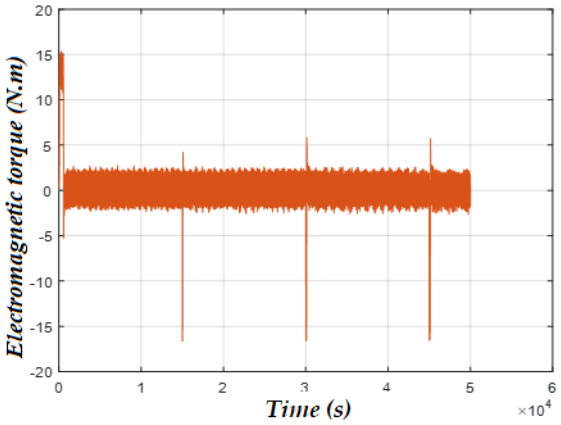

Figure IV. 3: Electromagnetic torque

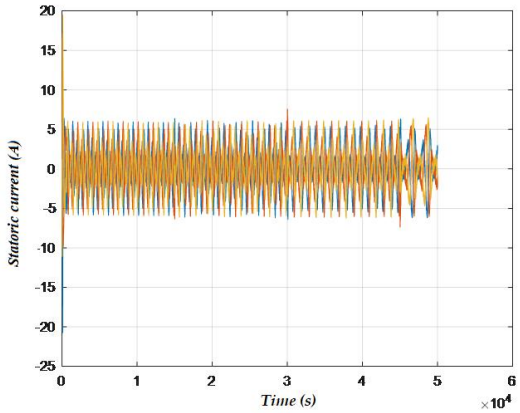

Figure IV. 4: Statoric currents

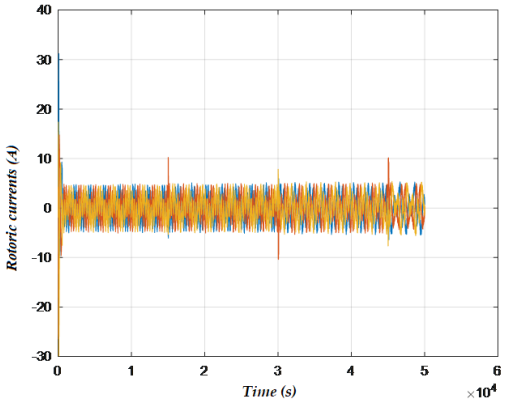

Figure IV. 5: Rotoric currents.

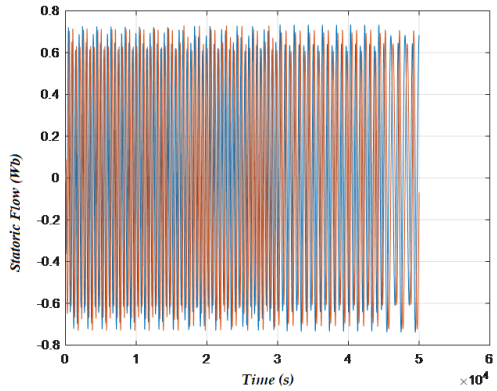

Figure IV. 6: Statoric Flow

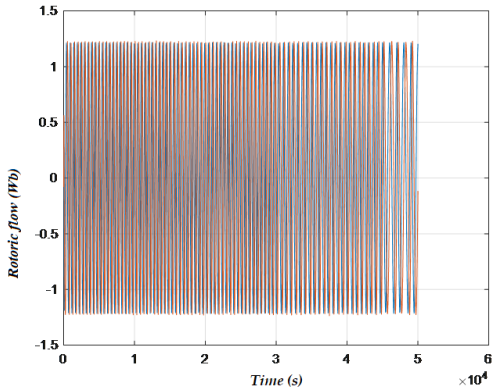

Figure IV. 7: Rotoric flow.

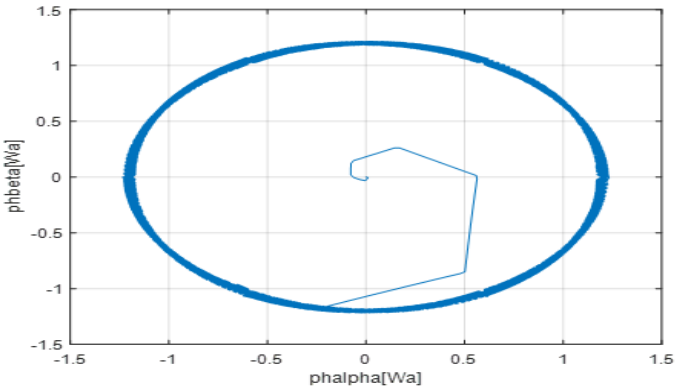

Figure IV. 8: Statoric flow (α; β).

IV.2.4. Interpretation of results:

We did the experiment in a vacuum in order to show the change in the reference velocity and its effect on the torque, as shown by the results of the simulation where we applied the instantaneous velocity where we applied a reference velocity of 125.6 at time 0, and values of (115.6; 105.6; 65.6) at instants (1.5; 3; 4.5) respectively. And we have obtained the velocity results as shown in Figure (IV.10) and these reference speeds have a momentary effect on the torque as shown in Figure (IV.9).

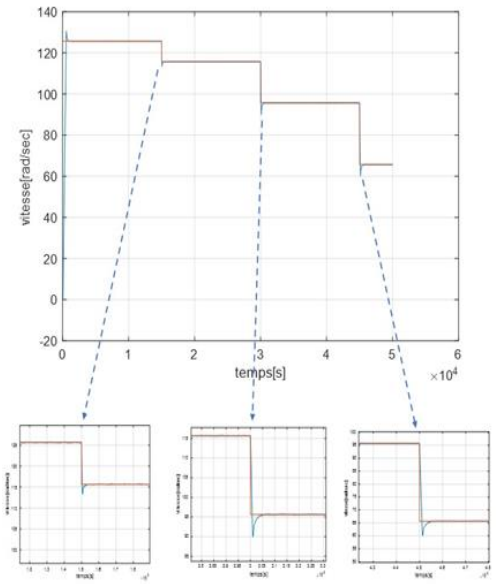

Figure IV. 10: Rotation speed

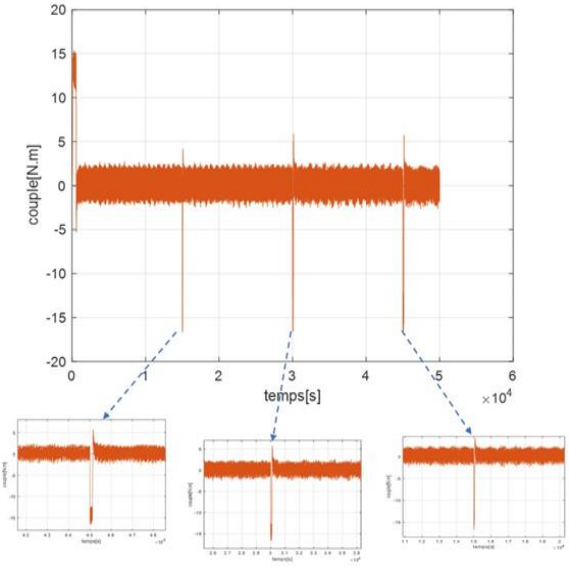

Figure IV. 9: Electromagnetic torque

IV.2.5. 1-charge start-up:

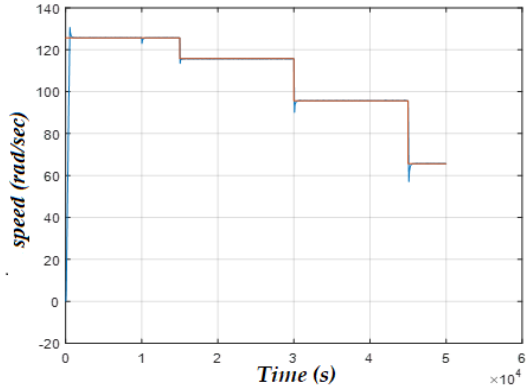

Figure IV. 11: Rotational speed

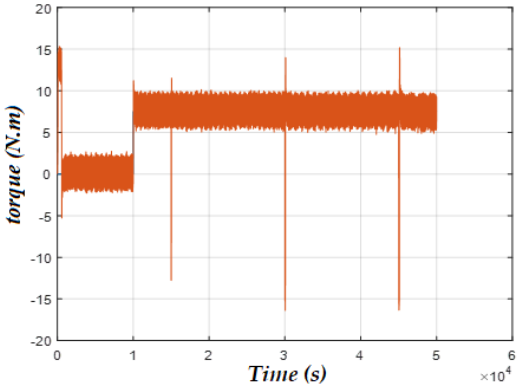

Figure IV. 12: Electromagnetic torque

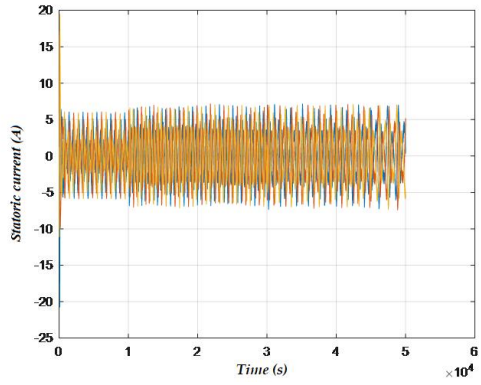

Figure IV.13: Statoric currents

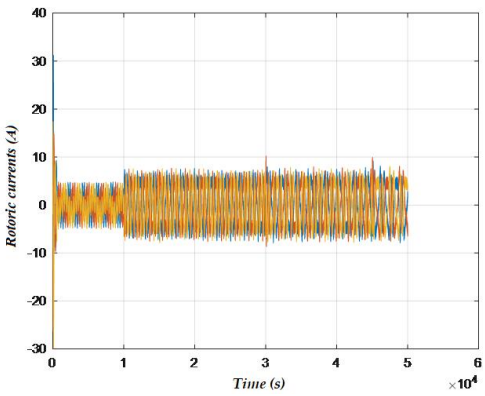

Figure IV. 14: Rotoric currents.

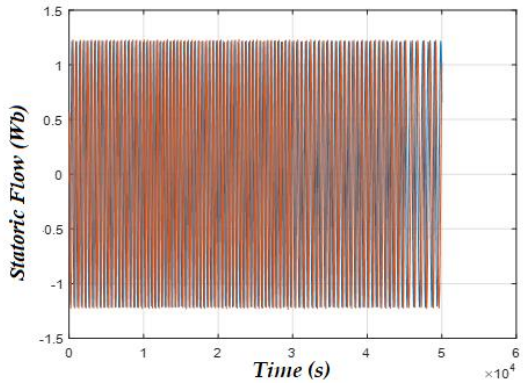

Figure IV. 15: Statoric Flow

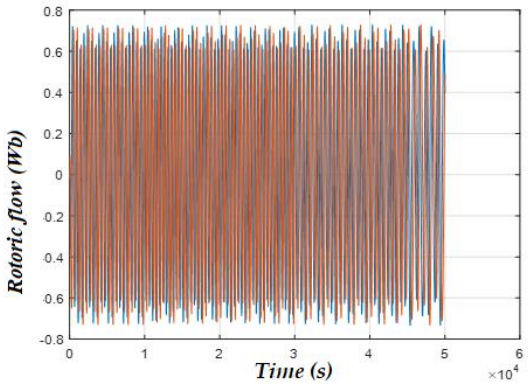

Figure IV. 16: Rotoric flow

IV.2.6. Interpretation of results:

It can be seen from this that the velocity has good dynamics, without transcendence or static error, and follows its reference in an acceptable manner. After the application of the resistive torque of a value of (12.5N.m to and t=1 s, as shown in Figure (IV.17) there is a very slight drop in velocity which subsequently returns to its reference value; this is due to the good performance of the speed control, When the resistance torque is applied, the electromagnetic torque is affected by its increase from the initial value as shown in Figure (IV.18).

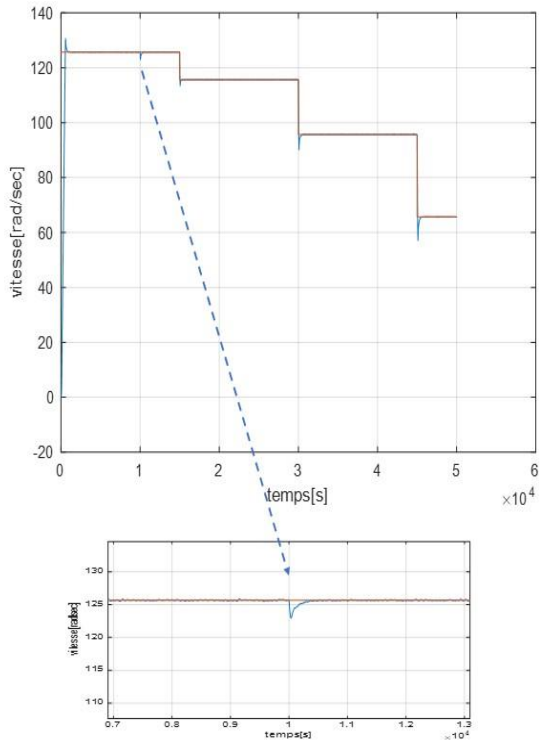

Figure IV. 17: Rotation speed

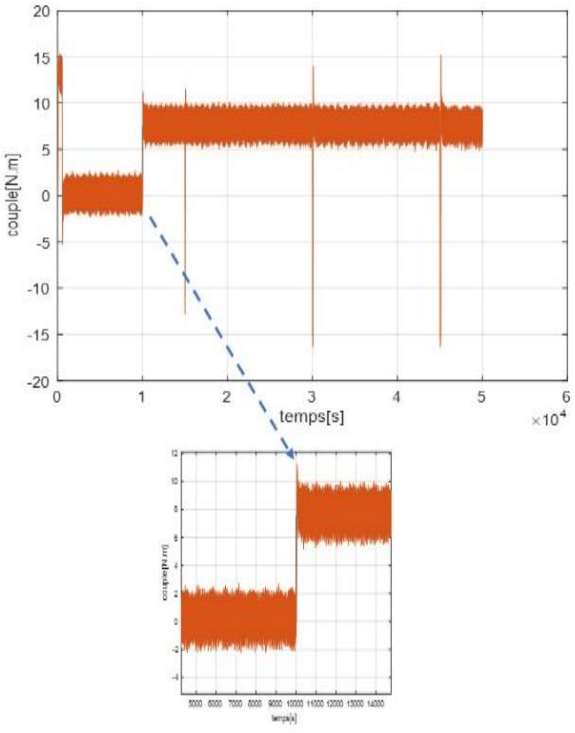

Figure IV. 18: Electromagnetic torque

IV.2.7. 3-charge start-up:

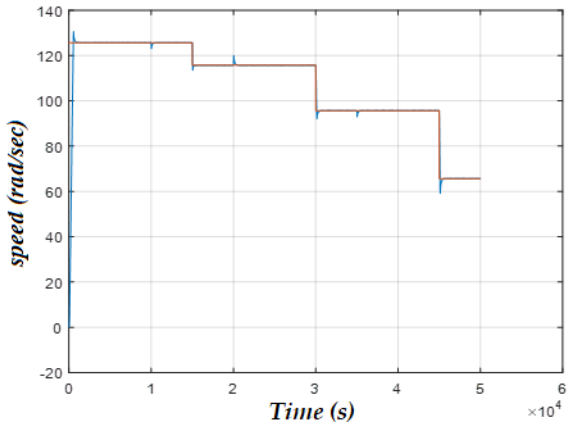

Figure IV. 19: Rotational speed

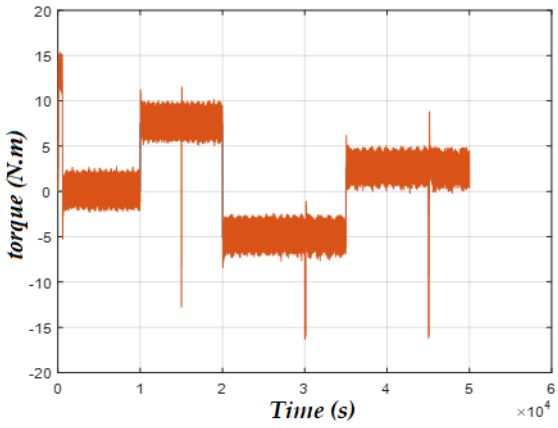

Figure IV. 20: Electromagnetic torque

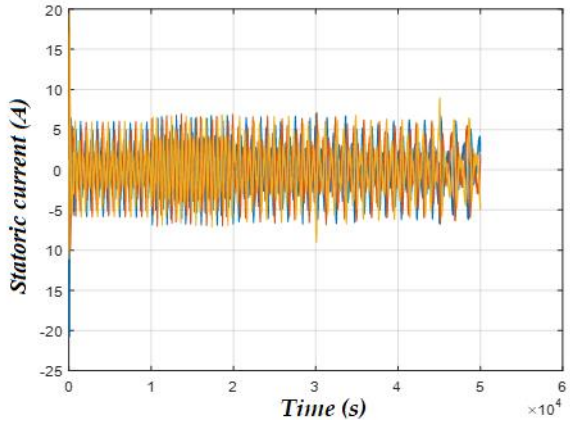

Figure IV.21: Statoric currents

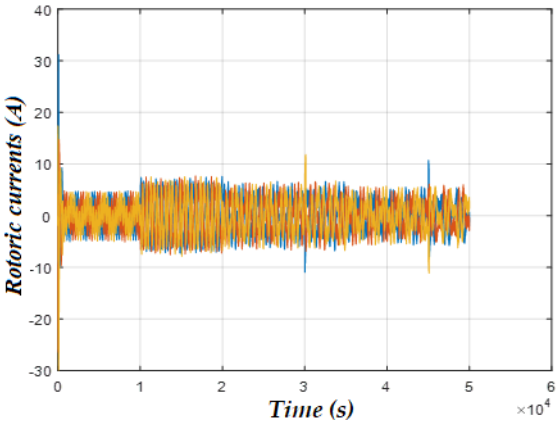

Figure IV. 22: Rotoric currents.

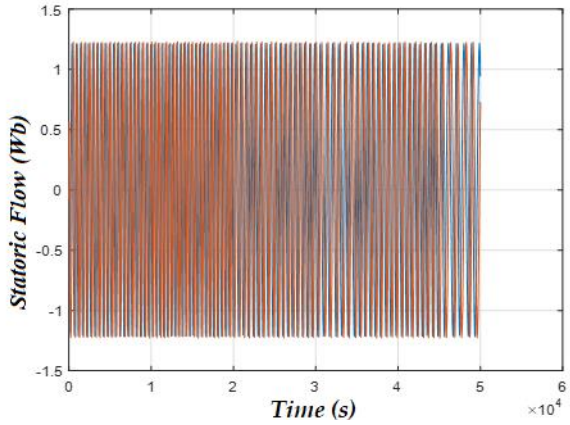

Figure IV. 23: Statoric Flow

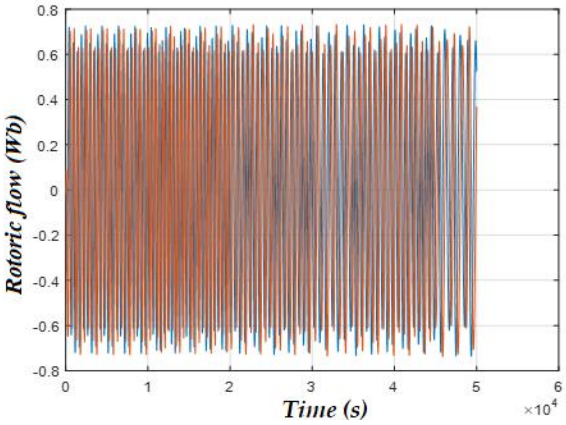

Figure IV. 24: Rotoric flow

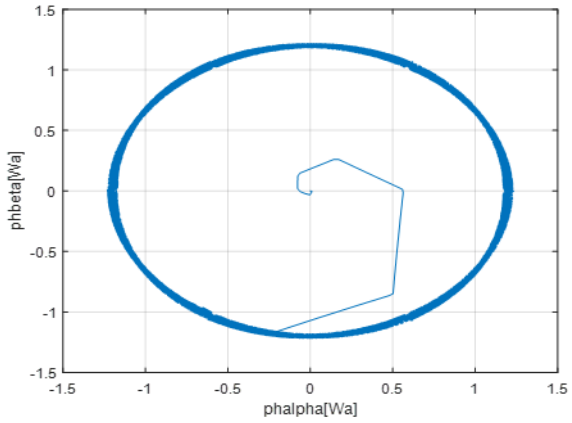

Figure IV. 25: Statoric flow (α; β).

IV.2.8. Interpretation of results:

It can be seen from this that the velocity has good dynamics, without transcendence or static error, and follows its reference in an acceptable manner. After the application of the resistive torque of a value of (12.5N.m to and -25 and 15) (t=1 s and 2 and 3), as shown in Figure (IV.26) there is a very slight drop in speed which subsequently returns to its reference value; this is due to the good performance of the speed control, When the resistance torque is applied, the electromagnetic torque is affected by its increase from the initial value as shown in Figure (IV.27).

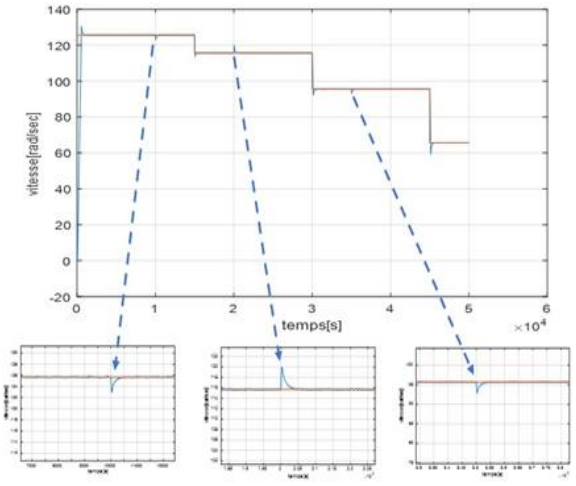

Figure IV. 26: Rotation speed

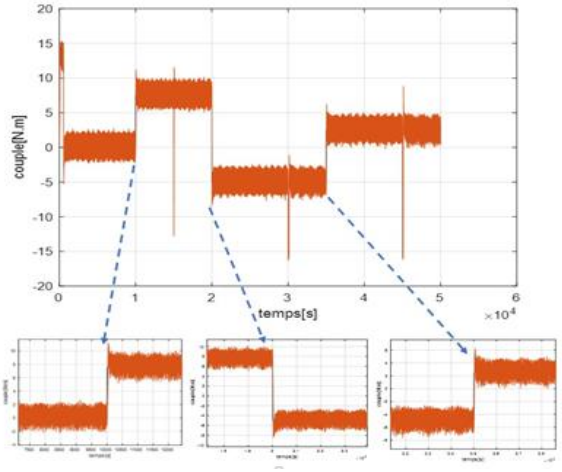

Figure IV. 27: Electromagnetic torque

IV.3. Conclusion

In this chapter, we have presented the structure of our study system. We detailed the order developed as well as the different steps followed to validate it by simulation.

The results thus obtained illustrate the proper functioning of our developed control. The use of MATLAB/Simulink simulation software allows us to model our system as faithfully as possible. Overall, the simulation results obtained are very satisfactory from the point of view of regulation, robustness and stability of the drive system under any operating conditions (vacuum, load, reversal of direction of rotation).

General Conclusion

GENERAL CONCLUSION

The asynchronous doubly fed machine is a non-linear, multi-variable system subject to parametric variations and unknown perturbations. After giving an overview of the DFIM, we focused on the modeling of the DFIM before presenting its dynamic model for commissioning. Subsequently, we explained the principle of direct torque control.

The study carried out in this delivery concerns the Direct Torque Control (DTC) of an asynchronous doubly fed machine as a solution to the problems encountered in the flow orientation vector control strategy. DTC is strong against parametric variations of the machine and does not require a position sensor. In addition, it offers a number of significant advantages over other types of control.

From this report and the simulation results obtained, the following conclusions can be drawn, which have been deemed to be of primary interest.

In addition to the development of various structures in electrical control and the appearance of various structures of power electronics converters, which now make it possible to have variable frequency power sources, the DFIM presents an ideal solution for high-power drives.

The study of electrical machines in general, and DFIM in particular, requires good mathematical modeling describing the entire machine and the system to be driven. This makes it possible to predict the dynamic and static performance of its drives

The DTC control technique applied to the DFIM can overcome the difficulty of its adjustment. It makes it possible to affirm the decoupling between the flux and the electromagnetic torque and improves the dynamics of the speed.

Finally, this work is an extension of the studies carried out on DFIM and needs to be continued in several directions.

Appendix

Appendix

Parameters of the doubly fed induction machine (DFIM)

RATED POWER: $P_n = 0.8\ kW$

NOMINAL STATOR VOLTAGE: $V_n = 220\ volts$

NOMINAL ROTOR VOLTAGE: $V_r = 15\ volts$

NOMINAL ROTOR VOLTAGE: $P = 2$

STATORICAL RESISTANCE: $R_s = 11.98\ \Omega$

ROTORIC RESISTANCE: $R_r = 0.904\ \Omega$

STATORIC INDUCTANCE: $L_s = 0.0414H$

ROTORIC INDUCTANCE: $L_r = 0.0556\ H$

MUTUAL INDUCTANCE: $M = 0.0.126\ H$

MOMENT OF INERTIA: $J = 0.01\ kg.\ m^2$

COEFFICIENT OF FRICTION: $f = 0.0001$

RATED SPEED: $N = 1420\ rpm$

NOMINAL FREQUENCY: $f = 50\ Hz$

Bibliography

Bibliography

[1] Mohammed Saci. Chabani, M. T. Benchouia, A. Golea, R. Boumaaraf. "Implementation of direct stator voltage control of stand-alone DFIGbased wind energy conversion system", 2017 5th International Conference on Electrical Engineering - Boumerdes (ICEE-B), 2017.

[2] M. El Ouanjli, A. Derouich, A. El Ghzizal, Y. El Mourabit, B. Bossoufi, and M. Taoussi, “Contribution to the performance improvement of doubly fed induction machine functioning in motor mode by the DTC control,” Int. J. Power Electron. Drive Syst., vol. 8, no. 3, pp. 1117–1127, 2017.

[3] S. Abderezak, «Contribution A La Commande Hybride :Mode Glissant - Floue De La Machine A Induction Double Alimentee,» Thèse Doctorat 3EME Universite Batna 2, 2021.

[4] Z. M. Yazid, «Contribution A La Commande D'UN Mada. Apport Des Techniques De L'intelligence Artificielle.,» These Doctorat Universite Batna 2, 2019

[5] F. Zidani, «La Commande Directe Du Couple De La Mada,» Memoire Master Universite Batna 2, Algria, 2020.

[6] M. Ahmed, M. K. Metwaly, and N. Elkalashy, “Performance investigation of multi-level inverter for DFIG during grid autoreclosure operation,” Int. J. Power Electron. Drive Syst., vol. 10, no. 1, p. 454, 2019

[7] Drid. S, Nait-Said. M.S, Tadjine. M, ‘‘Double Flux Oriented Control for the Doubly Fed Induction Motor Electric Power Components and Systems’’, Taylor & Francis Inc., 33:1081-1095, 2005.

[8] R. R. Behera and A. Thakur, “Finite-control-set predictive current control based real and reactive power control of grid-connected hybrid modular multilevel converter,” Int. J. Power Electron. Drive Syst., vol. 9, no. 2, pp. 660–667, 2018.

[9] H. Mesloub, M. T. Benchouia, A. Goléa, N. Goléa, and M. E. H. Benbouzid, “Predictive DTC schemes with PI regulator and particle swarm optimization for PMSM drive: comparative simulation and experimental study,” Int. J. Adv. Manuf. Technol., vol. 86, no. 9–12, pp. 3123–3134, 2016.

[10] Y.Djerir, «Commande Directe Du Couple Et Des Puissances D’une Mada Associee A Un Systeme Eolien Par Les Techniques De L’intelligence Artificielle,» These De Doctorat En Electrotechnique, Universite Djilali .

[11] S. Mensou, A. Essadki, T. Nasser, B. B. Idrissi, and L. Ben Tarla, “Dspace DS1104 implementation of a robust nonlinear controller applied for DFIG driven by wind turbine,” Renew. Energy, vol. 147, pp. 1759–1771, 2020.

[12] T. Riyadh, «Controle Des Puissances Generees Par Un Systeme Eolien A Vitesse Variable Base Sur Une Machine Asynchrone Double Alimentee,» These Doctorat L’Universi T Ebatna 2, 2016.

[13] S. Soued et al., “Experimental behaviour analysis for optimally controlled standalone DFIG system,” IET Electr. Power Appl., vol. 13, no. 10, pp. 1462–1473, 2019.

[14] S. Soued, M. A. Ebrahim, H. S. Ramadan, and M. Becherif, “Optimal blade pitch control for enhancing the dynamic performance of wind power plants via metaheuristic optimisers,” IET Electr. Power Appl., vol. 11, no. 8, pp. 1432–1440, 2017.

[15] B. B. M. El Amine, A. Ahmed, M. B. Houari, and D. Mouloud, “Modeling, simulation and control of a doublyfed induction generator for wind energy conversion systems,” Int. J. Power Electron. Drive Syst., vol. 11, no. 3, pp. 1197–1210, 2020.

[16] B. Youcef, «Etude Et Commande Du Moteur Asynchrone A Double Alimentation (Mada) Par Differentes Techniques Avancees,» Memoire Magister Universitaire D’el-Oued, 2010

[17] Jaladi, K.K., Sandhu, K.S. & Bommala, P. Real-Time Simulator of DTC–FOC-Based DFIG During Voltage Dip and LVRT. J Control Autom Electr Syst 31, 402–411 (2020).

[18] Y. Bekakra, «These Presentee En Vue De L’obtention Du Diplome De Doctorat En Sciences Contribution A L’etude Et A La Commande Robuste D’un Aerogenerateur Asynchrone A Double Alimentation,» These Doctoratuniversite Mohamed Khider – Biskra, 2014.

[19] Paweł Maciejewski Et Grzegorz Iwański, «Six-Phase Doubly Fed Induction MachineBased Standalone Dc Voltage Generator,» Bulletin Of The Polish Academy Of Sciences, Vol. 69, P. 10, 2021.

[20] Arezki Chibah Et Madjid Meziani, «Commande Directe Du Couple (Dtc) D’un Moteur Asynchrone A Double Alimentation.,» Universite De Mouloud Mammeri De Tizi Ouzou, Algria, 2013.

[21] G. Abad, M. A. Rodriguez, and J. Poza, "Two-level VSC based predictive direct torque control of the doubly fed induction machine with reduced torque and flux ripples at low constant switching frequency, " IEEE Transactions on Power Electronics. vol. 23, no. 3, pp. 1050–1061, May 2008.

[22] R. Tirumala and N. Mohan, "Seamless transfer of a grid-connected PWM inverters between utility-interactive and stand-alone modes," in Proceedings Annual Power Electronic Conference, vol. 2, pp. 1081–1086, 2002.

[23] S. A. Gomez and J. L. R. Amenedo. "Grid synchronization of doubly fed induction generators using direct torque control," IEEE 28th Annual Conference of the Industrial Electronics Society, pages 3338–3343, 2002.

[24] R. Datta, and V.T. Ranganathan, "Direct power control of grid-connected wound rotor induction machine without rotor position sensors," IEEE Transactions on Power Electronics, vol. 16, no. 3, pp.390–399, May 2001.

[25] M. Dybkowski, K. Szabat, Direct Torque Control of Induction Motor Drive System with Adaptive Sliding-Mode Neuro-Fuzzy Compensator, in: IEEE Int. Conf. Ind. Technol., 2015: pp. 714–719.